

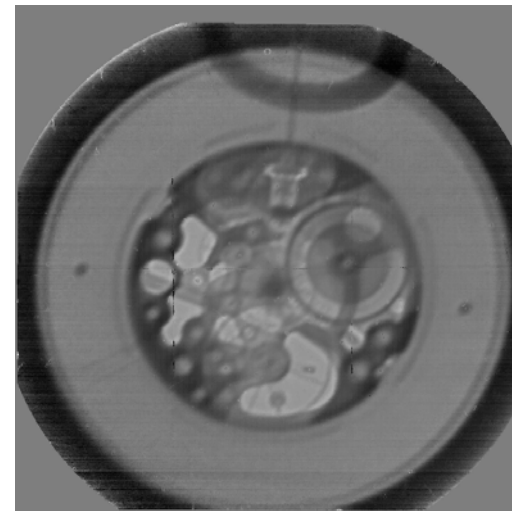
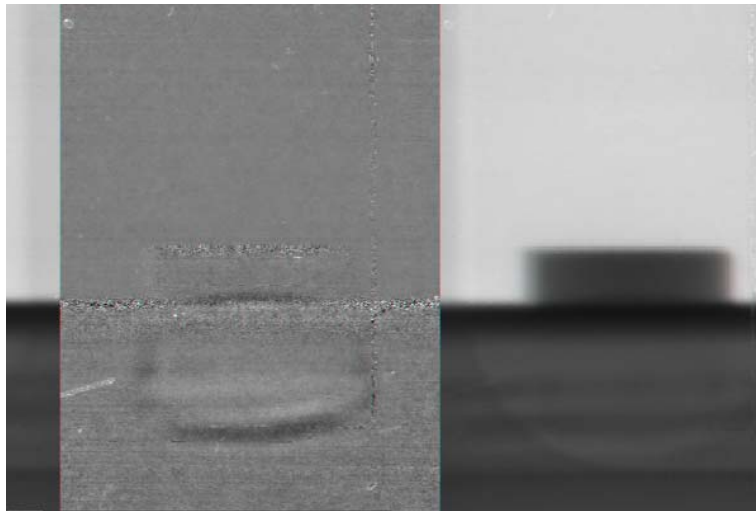
UNCLASSIFIED

Proton Radiography: Studying Dynamic Properties of Shock-Loaded Materials

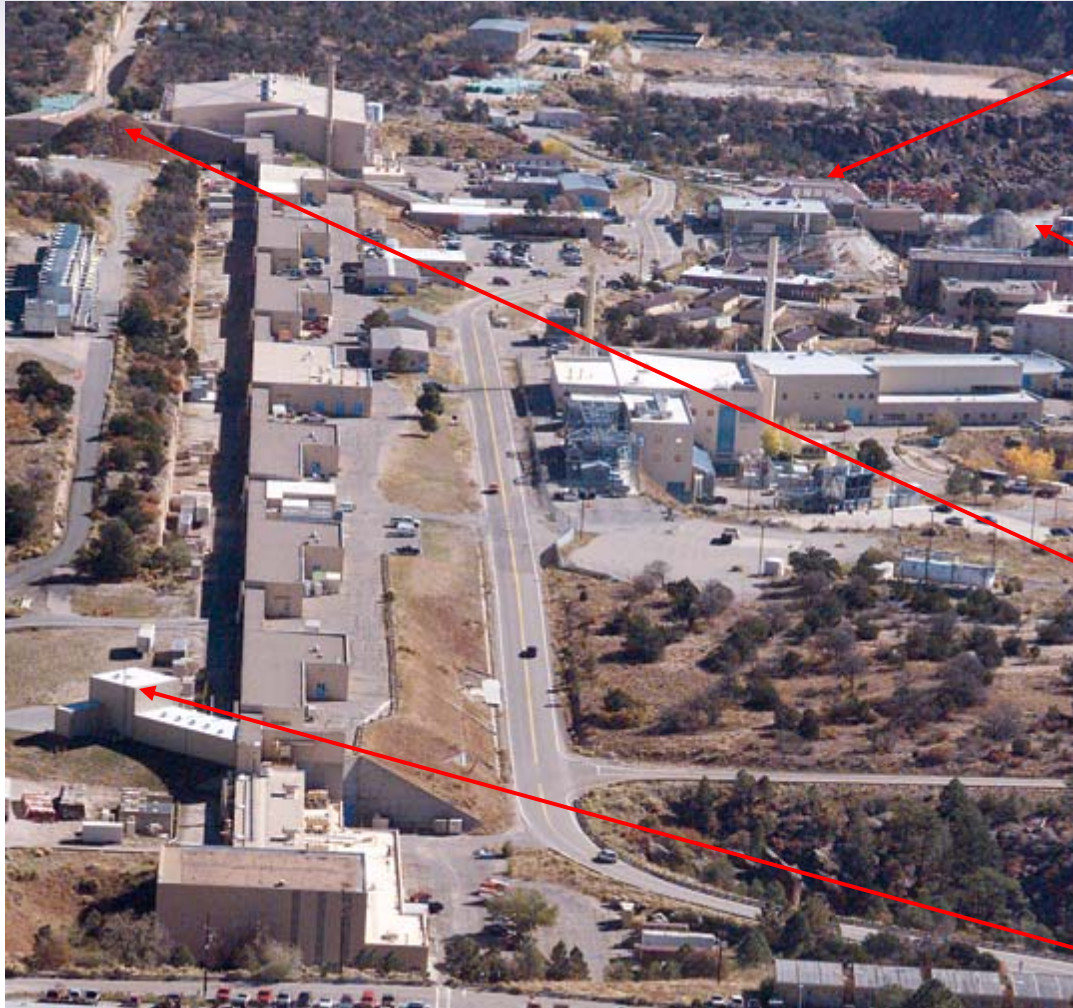
Cynthia L. Schwartz
and the pRad Collaboration
Physics Division
Los Alamos National Laboratory

5×10^6 Hz
800 MeV p

2 Hz
800 MeV p



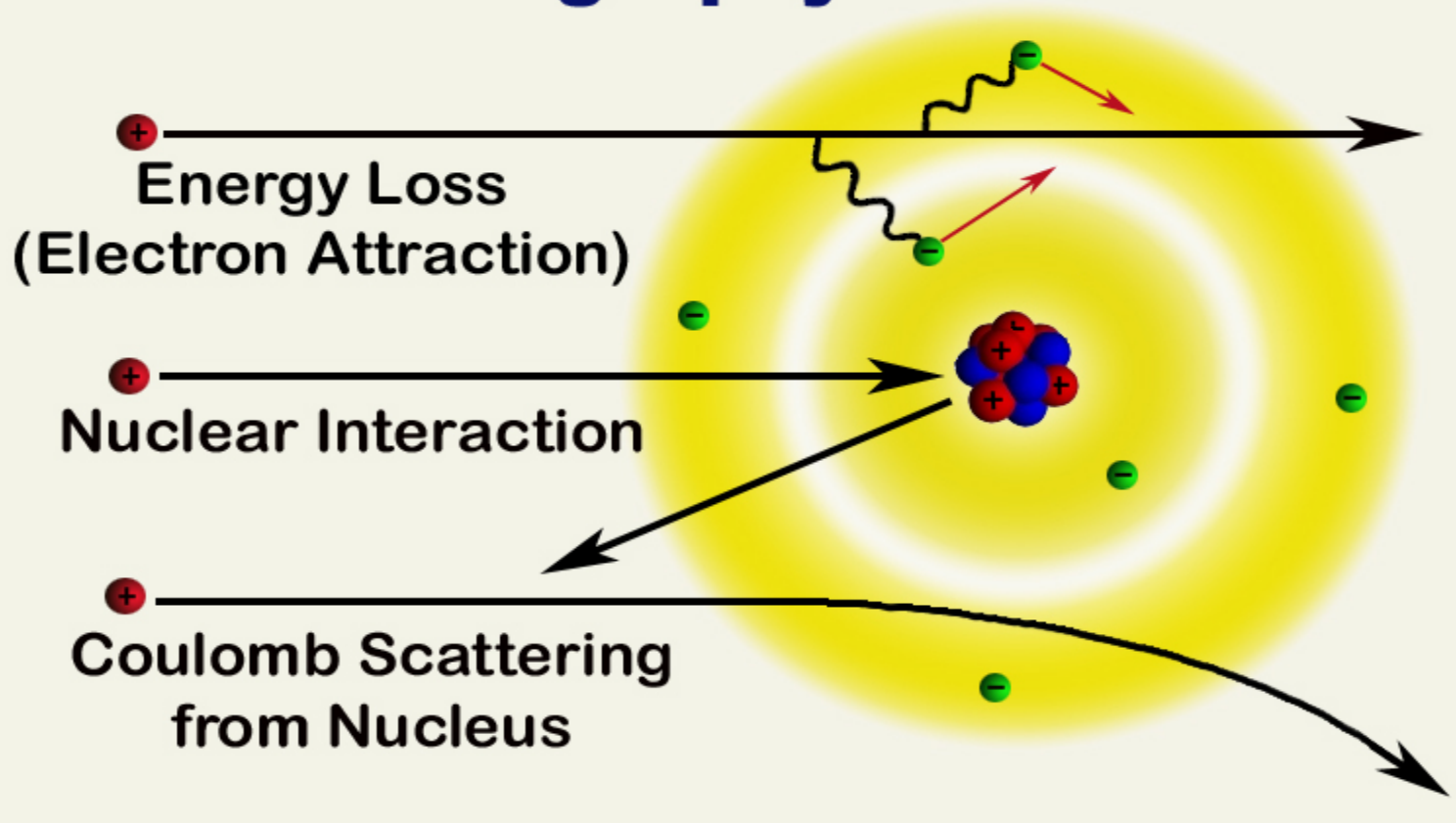
LANSCÉ Experimental Areas



- Lujan Center
 - *National security research*
 - *Materials, bio-science, and nuclear physics*
 - *National user facility*
- WNR
 - *National security research*
 - *Nuclear Physics*
 - *Neutron Irradiation*
- Proton Radiography
 - *National security research*
 - *Dynamic Materials science,*
 - *Hydrodynamics*
- Isotope Production Facility
 - *Medical radioisotopes*

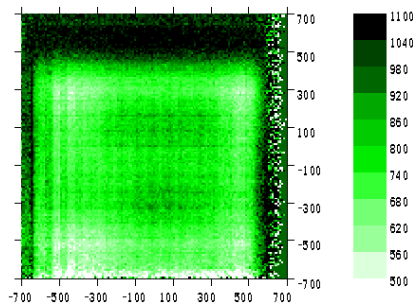
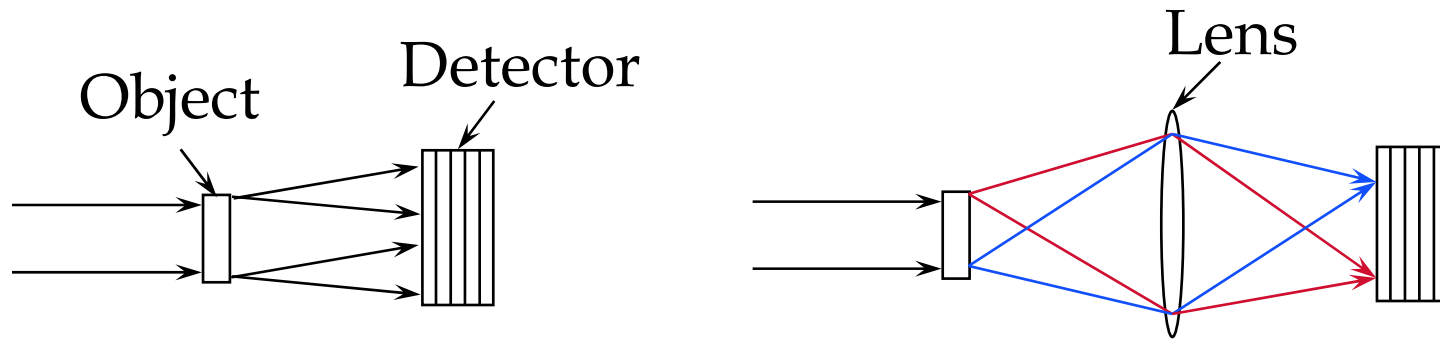
Proton Interactions

Proton Radiography

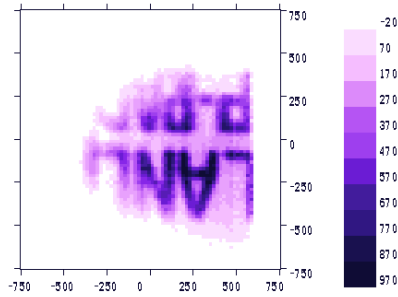


The idea-focus the transmitted protons with magnetic lenses

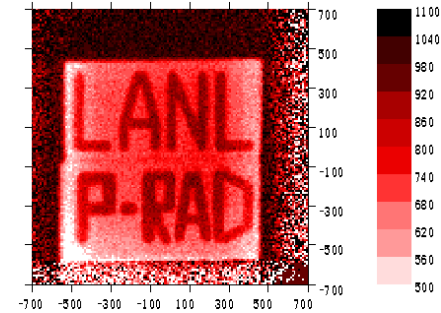
Transmission radiography FY95 with 188 MeV protons



At the detector

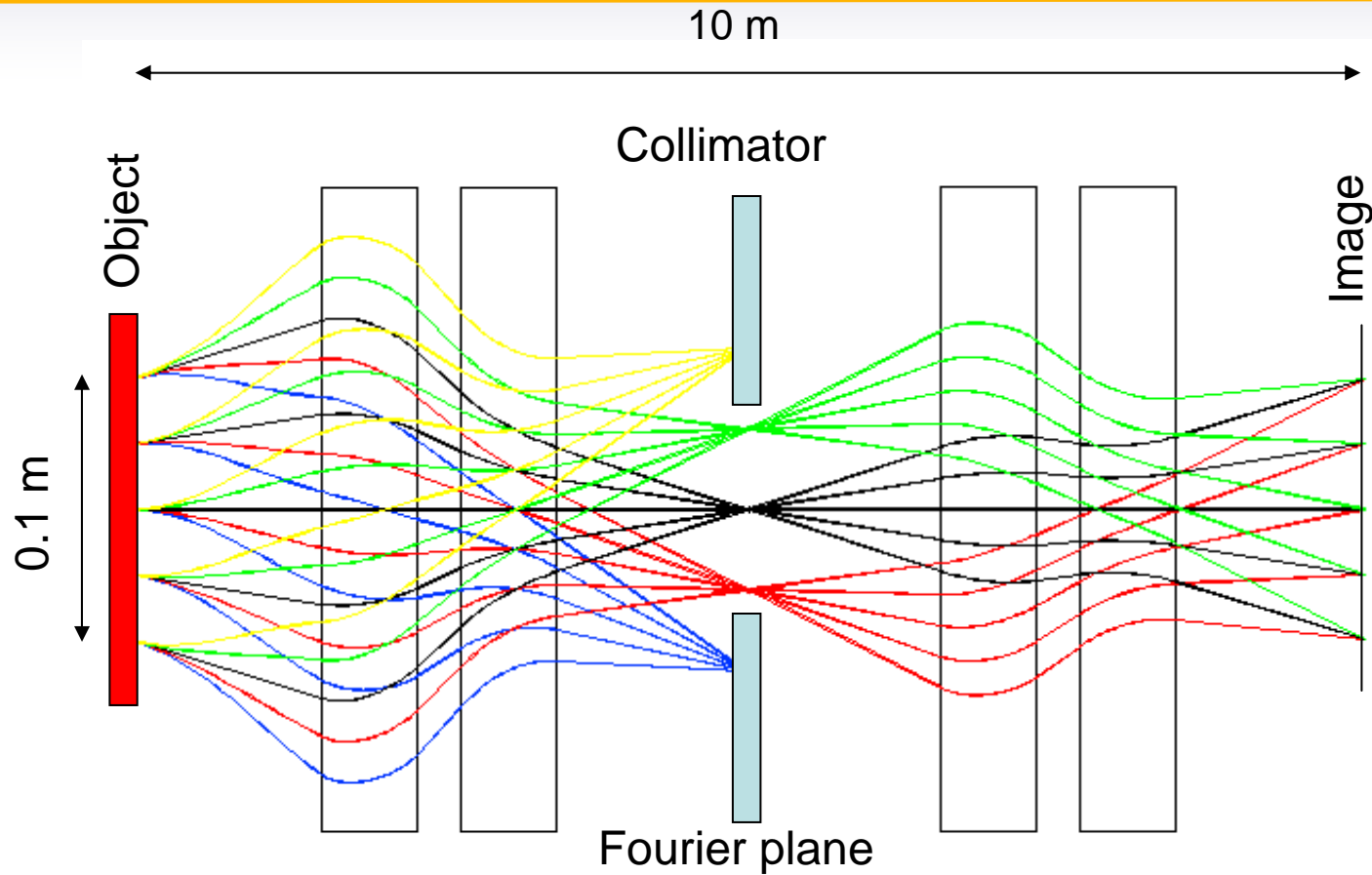


After a lens

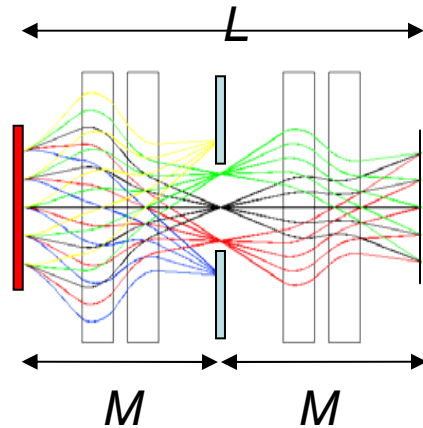


Projected to the object

Magnetic Imaging Lens



“Matching Miracle”



- x_o, x_o' - position and angle at object
- x_{fp} - position at midpoint of lens
- x_i - position and angle at image
- δ - $\Delta p/p$
- M - Transport matrix for doublet
- L - First order Transport matrix
- T - Second order Transport tensor

$$L = M^2 = -I$$

Fourier Plane

$$x_{fp} = M_{11}x_o + M_{12}x_o'$$

$$x_o' = wx_o + \phi$$

$$x_{fp} = M_{11}x_o + M_{12}(wx_o + \phi)$$

$$w = -M_{11}/M_{12}$$

$$x_{fp} = M_{12}\phi$$

Resolution

$$x_i = L_{11}x_o + L_{12}x_o' + T_{116}x_o\delta + T_{126}x_o'\delta$$

$$x_i = -x_o + T_{116}x_o\delta + T_{126}(wx_o + \phi)\delta$$

$$w = -T_{116}/T_{126} = -M_{11}/M_{12} *$$

$$w = -M_{11}/M_{12}$$

$$\Delta x_i = T_{126}\phi\delta$$

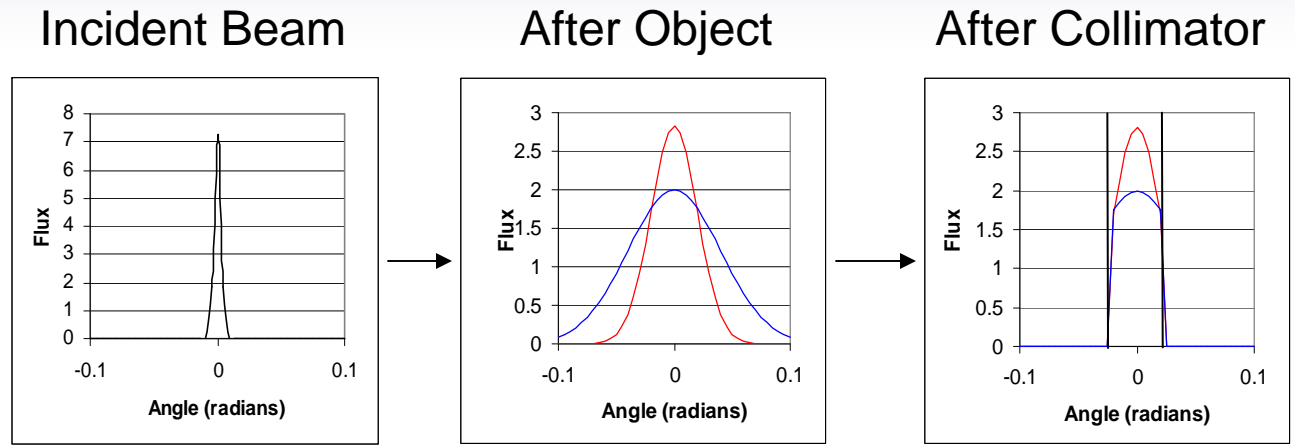
Dominates Blur

Form identity lens from identical doublets

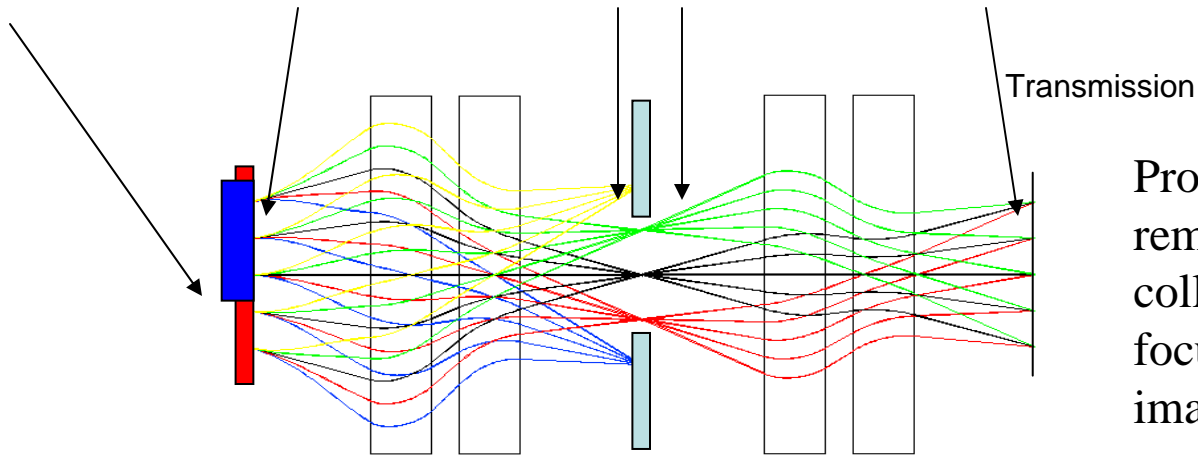
Inject beam with position-angle correlation to form Fourier plane at center of lens.

Same position-angle correlation which forms a Fourier plane at the center of the magnet also cancels second order chromatic terms.

Contrast from Multiple Coulomb Scattering



Measured transmission provides information of object thickness



Protons not removed by collimator are re-focused at the image location.

Areal Density Reconstruction

$$T_{nuclear} = e^{-x/\lambda}$$

Nuclear removal processes

$$T_{MCS} = 1 - e^{-\theta_o^2 / 2x}$$

Multiple Coulomb Scattering with collimation:

$$\theta_o = \frac{14.1 \text{ MeV}}{p\beta} \sqrt{\frac{x}{x_o}}$$

θ_o - scattering angle (radians)

x - areal density

x_o - radiation length

p - momentum (MeV)

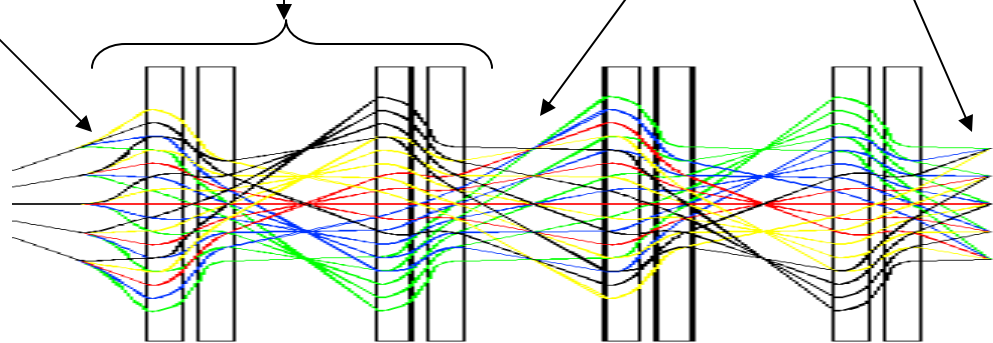
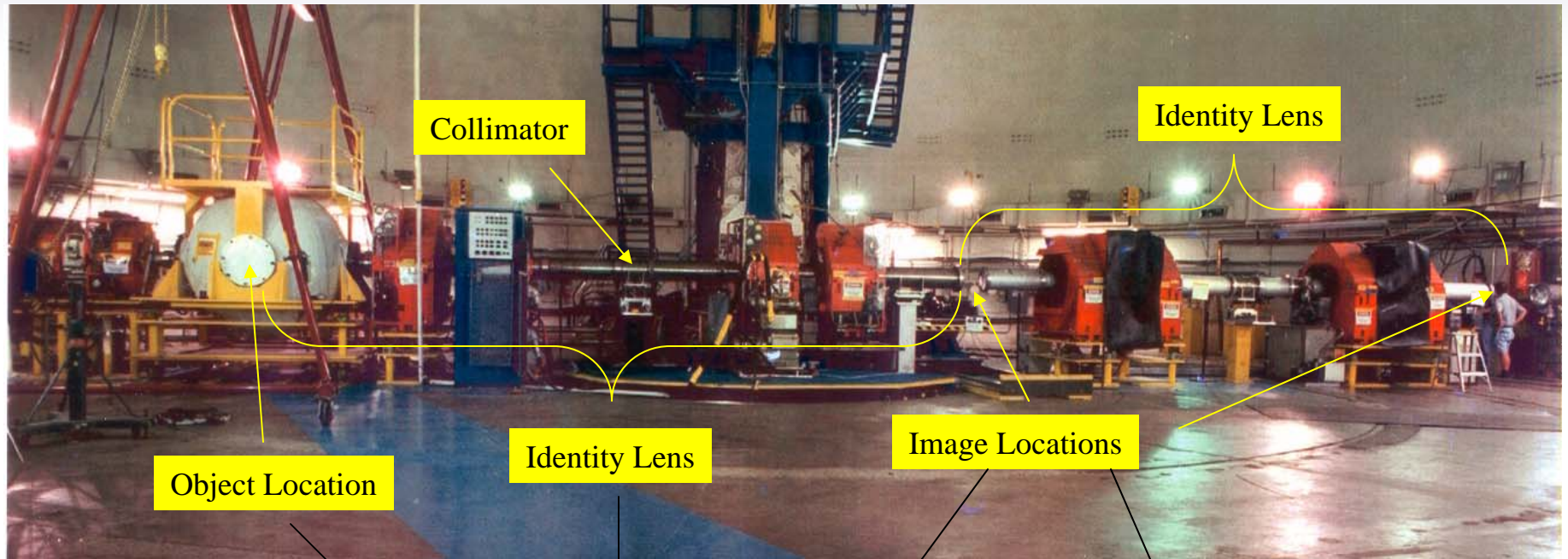
β - relativistic velocity

$$T = e^{-x/\lambda} \left(1 - e^{-\left(\frac{\theta_o p \beta}{14.1 \text{ MeV}}\right)^2 \frac{x_o}{2x}} \right)$$

Total Transmission

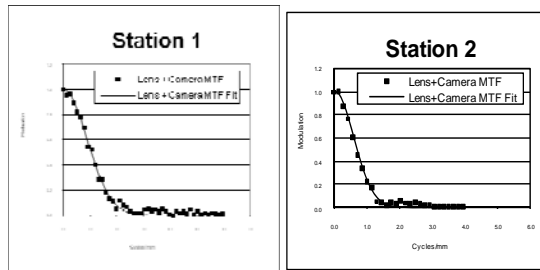
- inverted to determine areal density, x

pRad Facility at LANSCE



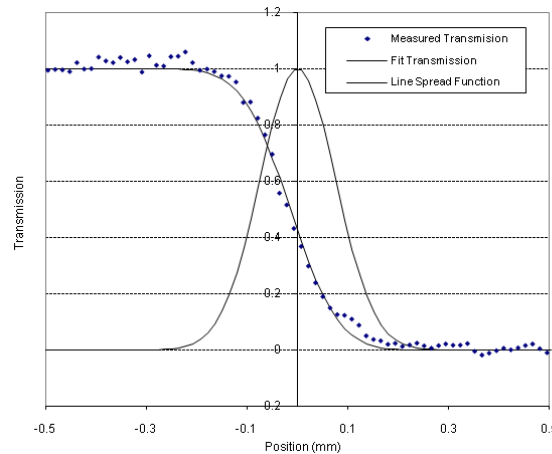
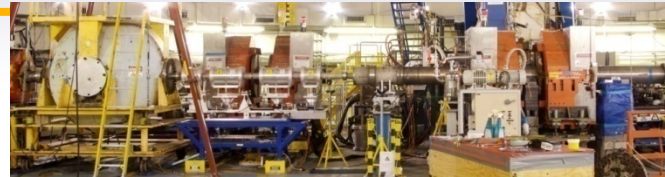
800 MeV Spatial Resolution

Identity Lens

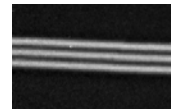


- Station 1: 178 μm
- 120 mm field of view

X3 Magnifier

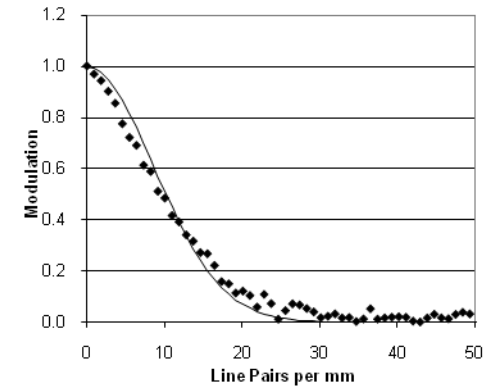
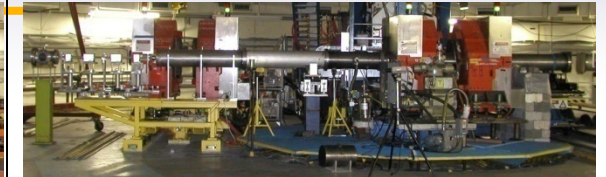


2.5 lp/mm



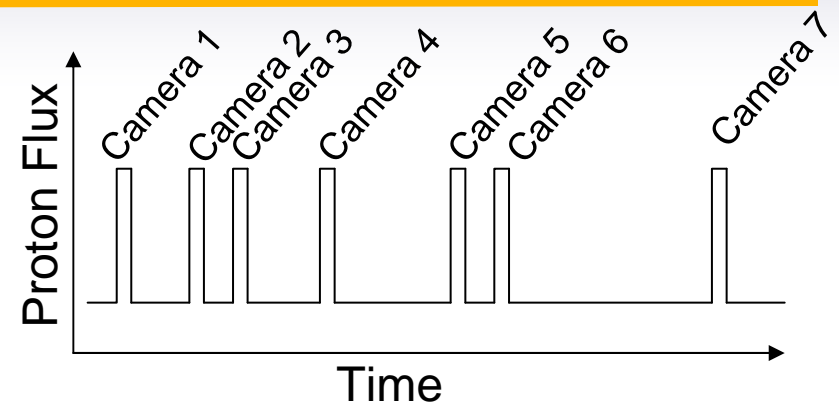
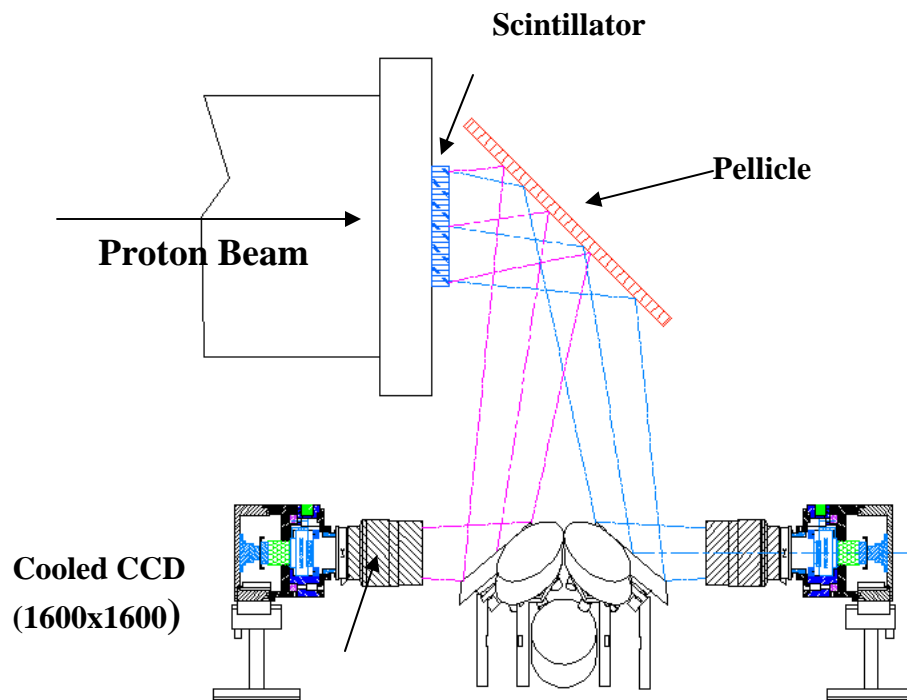
- Station 1: 65 μm
- 44 mm field of view

X7 Lens



- Station 1: 30 μm
- 17 mm field of view

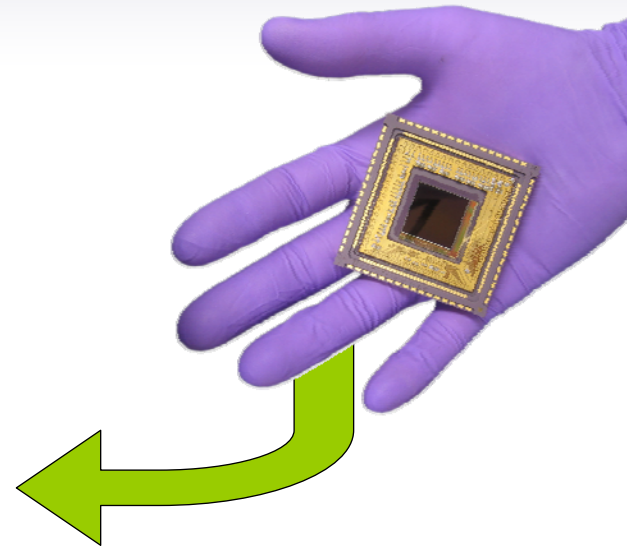
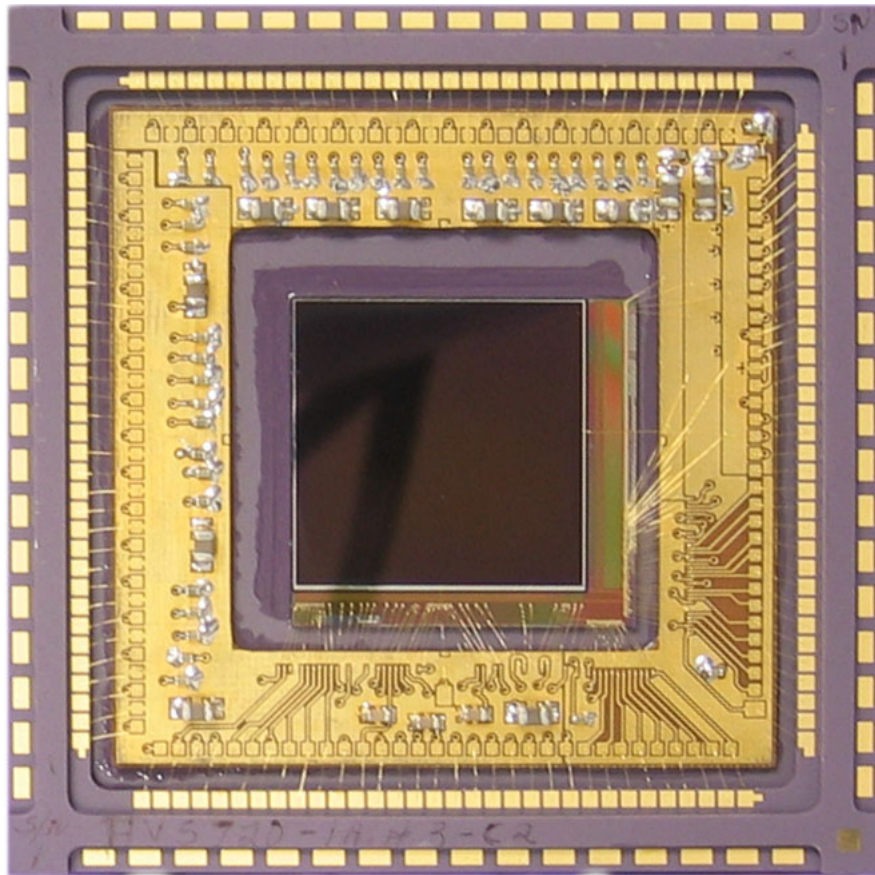
Temporal Resolution



- **19** images at first station
- **22** images at second station
- Total **41** possible image times
- Typically **50 ns** exposure times

3 Frame
Camera on a
Chip (720x720)

First 720×726-Pixel Hybrid Chip



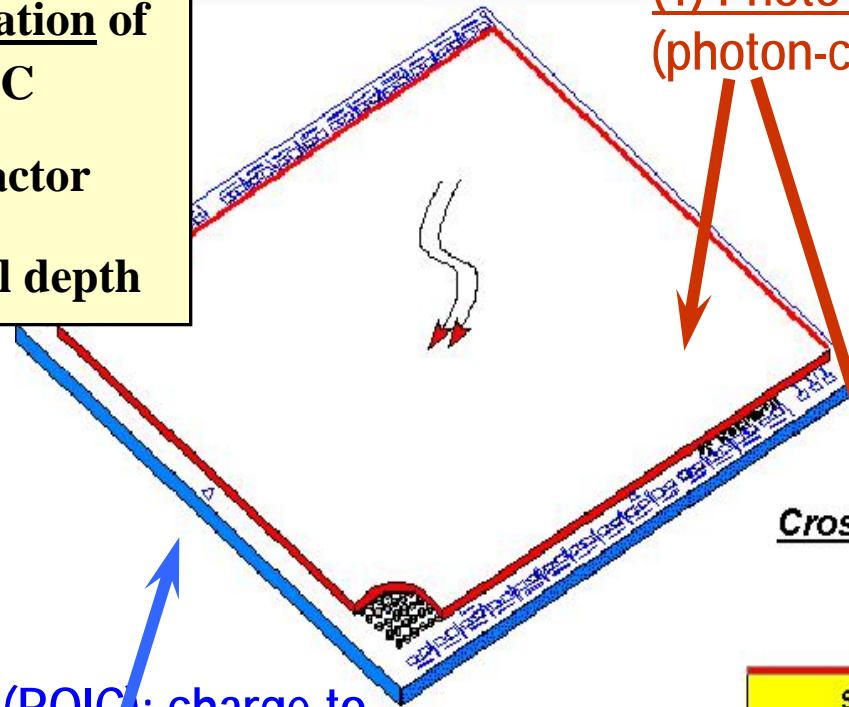
- Packaged prototype is a single 720×720 px FPA
- 1440×1440 imager can use a 2-side buttable 720×726 FPA in a Tiled Assembly
- On and off-chip decoupling with multiple wire-bonds to dampen large power transients

Imager as Two-Component Hybrid Focal Plane Array (FPA)

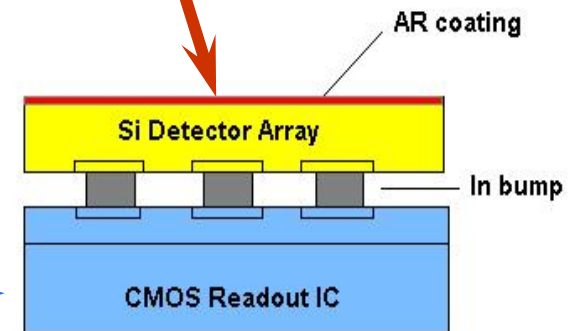
- **Independent optimization of detector and readout IC**
- **~100% optical fill factor**
- **Arbitrarily large well depth**

(1) **Photo-Diode Pixel Array**
(photon-charge conversion)

(2) **CMOS Readout IC (ROIC):** charge-to-voltage conversion, signal storage & processing, logic and A/D conversion;
SoC: photons-to-bits



Cross-Sectional View



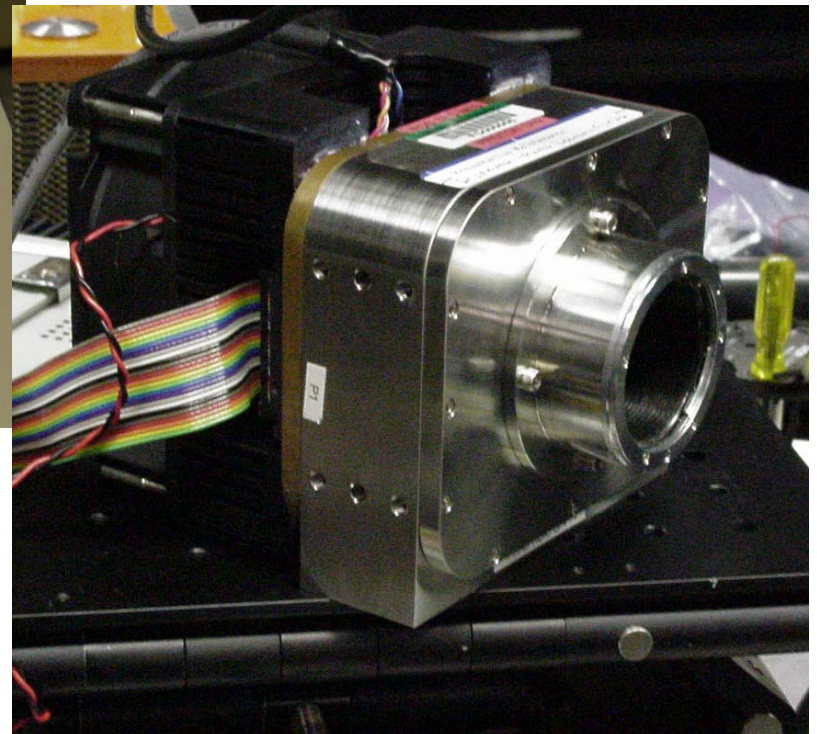
Each pixel in PD Sensor Array bump bonded to corresponding pixel in ROIC

Rockwell/ Teledyne pRAD Cameras



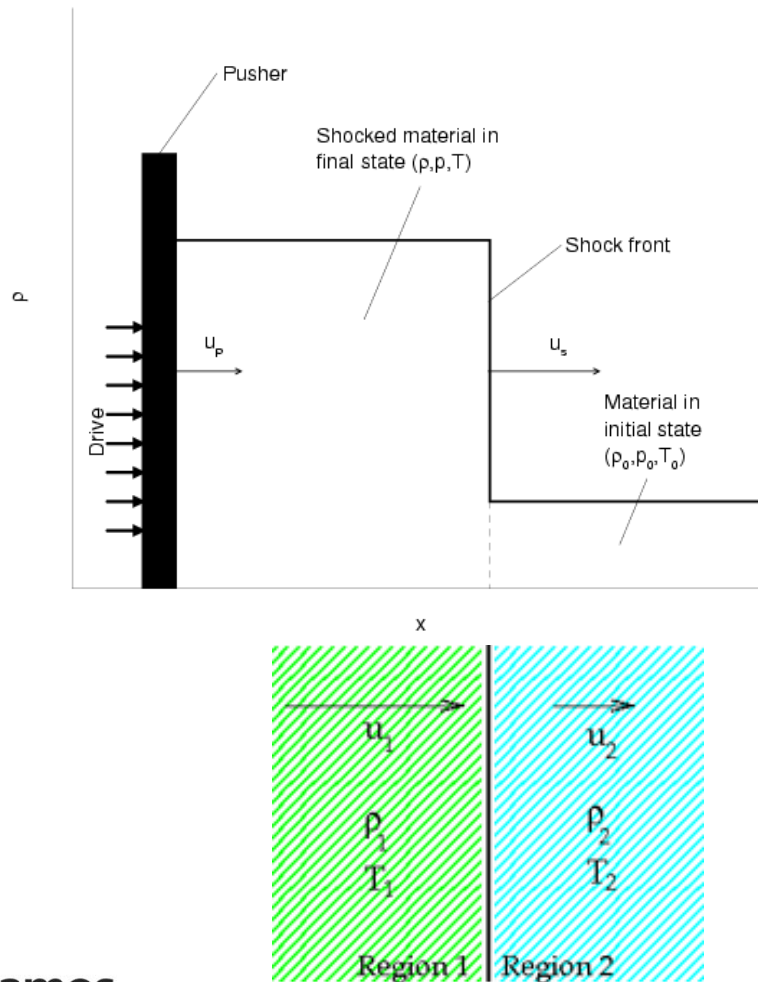
Prototype –in Al housing

(Sizable volume taken-up by TEC cooler and fan)



Stainless-Steel Dewar

What is a principal Hugoniot?

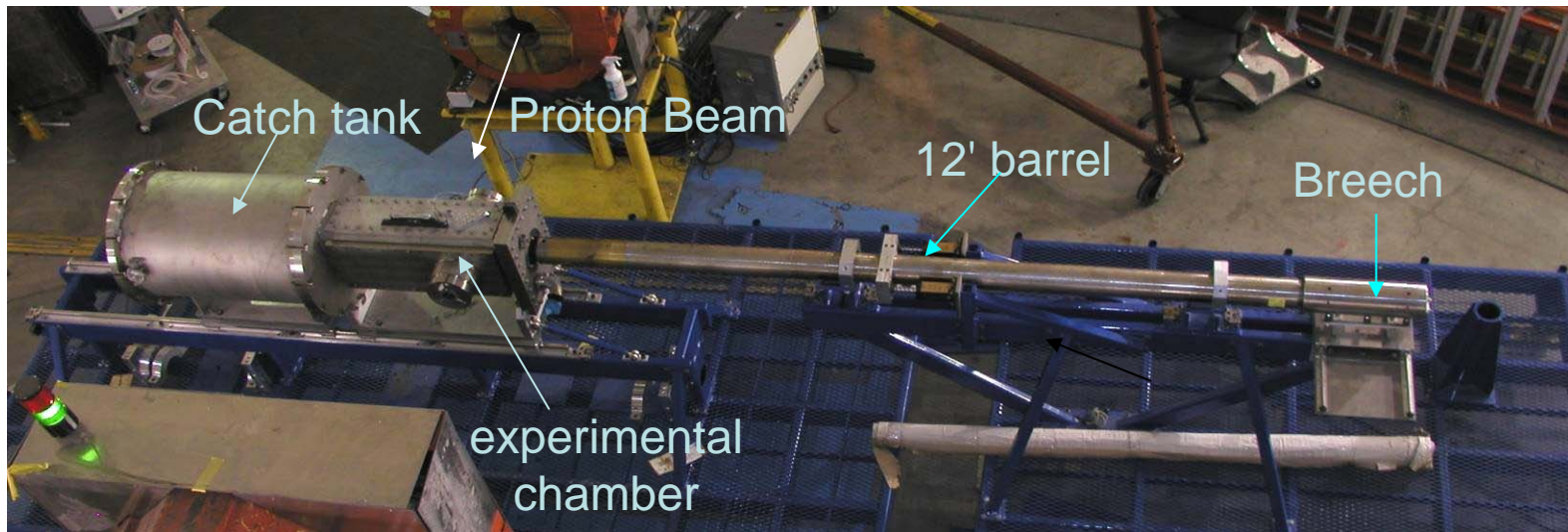


- locus of all final states characterized by (ρ , P , T)
- Conservation of mass, momentum, and energy result in pressure and density relations:

$$p - p_0 = \rho_0 u_s u_p$$

$$\rho / \rho_0 = u_s / (u_s - u_p)$$

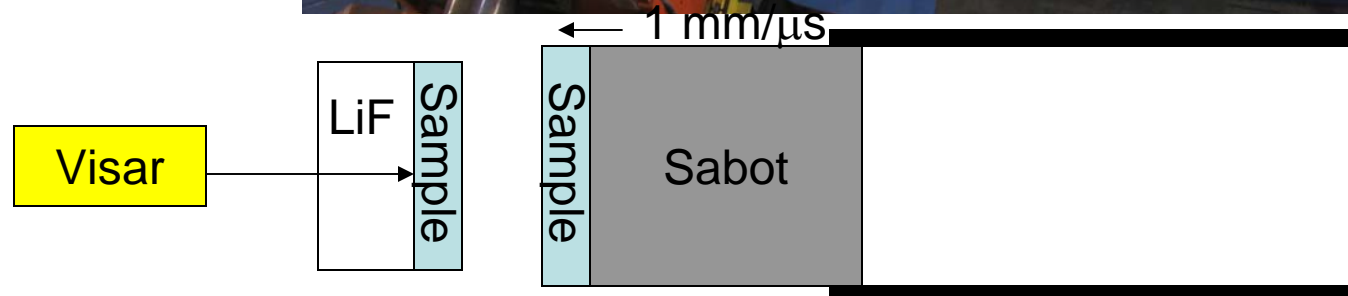
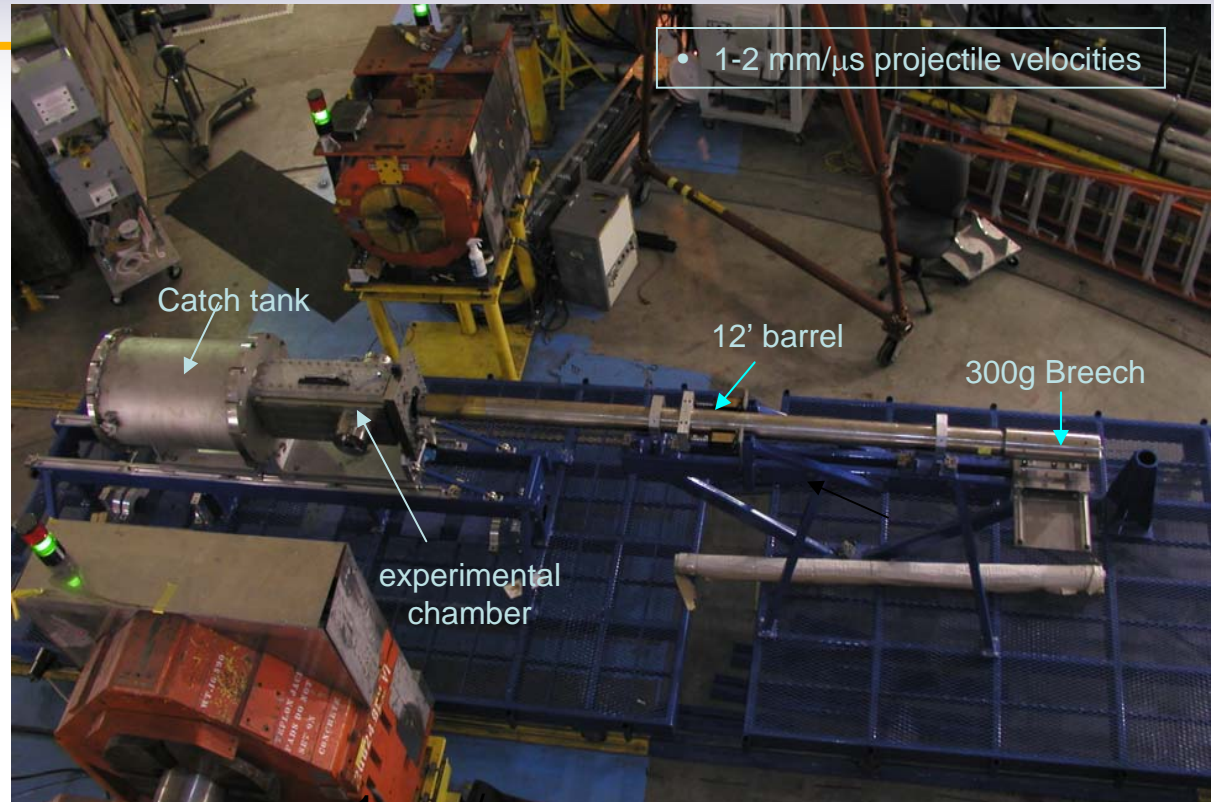
Investigation of Dynamic Phase Transitions in Metals using the 40mm Launcher in Area C - Continued



P. A. Rigg, C. L. Schwartz, F. J. Cherne, G. T. Gray III

Powder Gun Coupled with pRad

- 1-2 mm/ μ s projectile
- Planar drive
- Synchronized to proton pulses
- Supported shock wave



UNCLASSIFIED

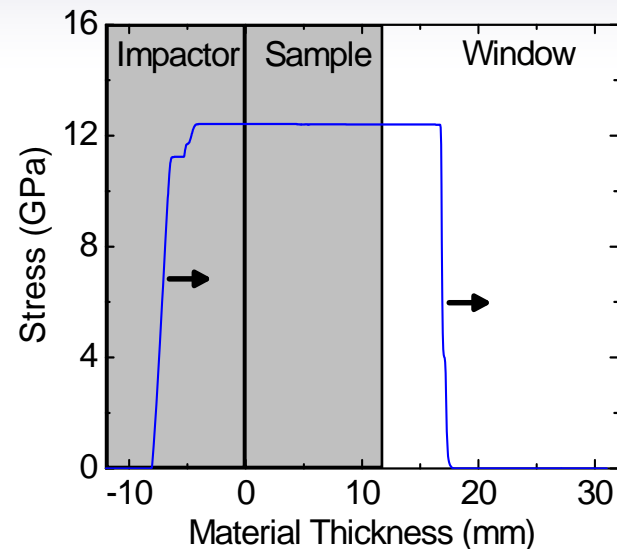
Motivation

- Density measurements with 0.5% to 2% accuracy needed to develop accurate equations of state
- Direct density measurement techniques and data are lacking
 - Calculated values can have unacceptably large error
 - Quantitative Dynamic X-Ray Diffraction data currently limited to single crystals
 - X-Ray radiography limited to a few snapshots per experiment
- Plate impact technique provides well-characterized 1-D shock loading to samples
- PRAD can provide both direct density measurements and resolution of mesoscale feature with many frames of data per experiment
- Can coupling provide quantitative, real-time measurements of meso-scale processes for the first time? Can accurate density measurements behind shock front be achieved?

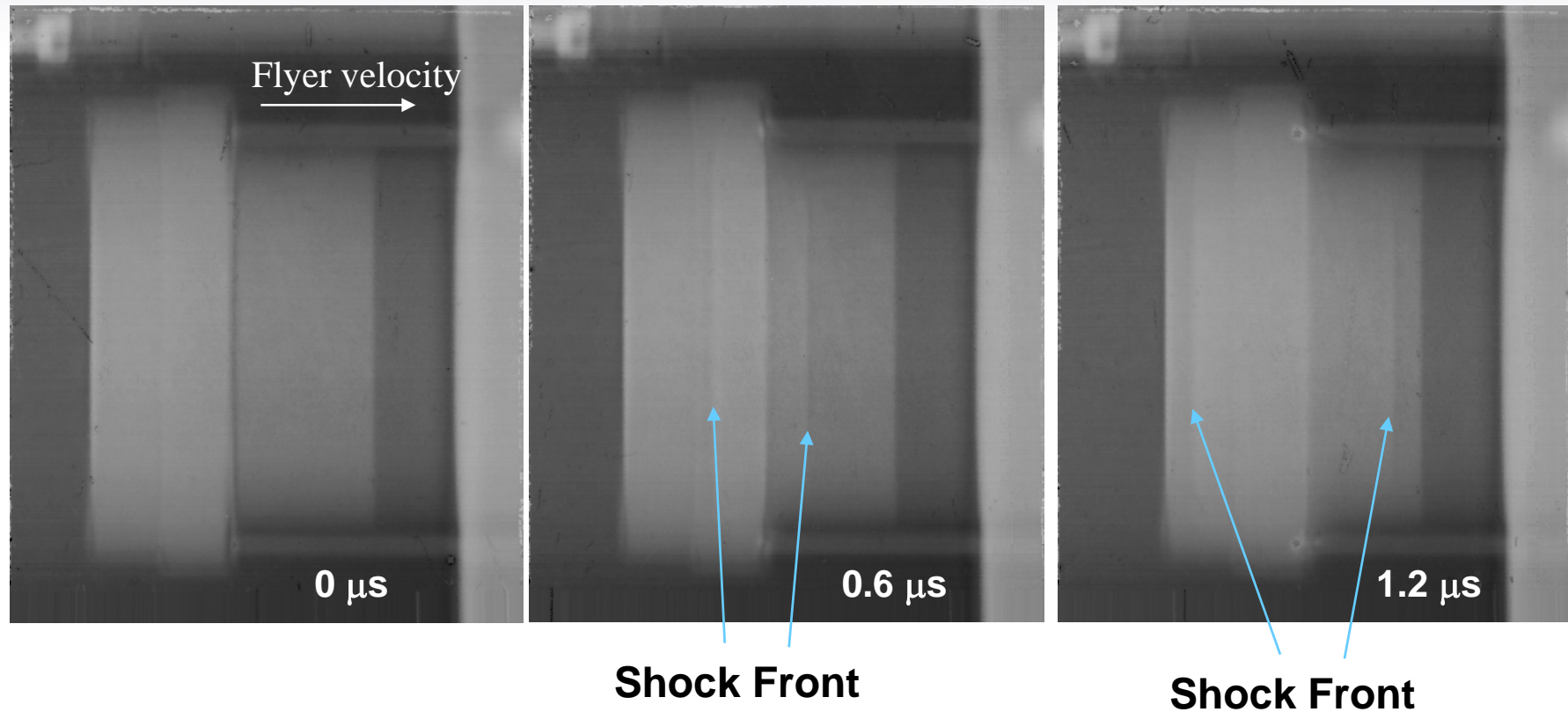
Density Measurements in Aluminum and Copper

- Four symmetric impact experiments were completed
 - Two experiments on 6061-T6 Aluminum
 - Two experiment on OFHC Copper
 - All samples backed by LiF window to maintain stress at back
- High confidence in EOS for Aluminum and Copper
- Calculate density using Jump Conditions given $P(u_P)$ and measured projectile velocity, u_0

$$u_P = \frac{1}{2}u_0 \quad P = \rho_0 U_S u_P \quad \rho = \frac{\rho_0 U_S}{U_S - u_P}$$



Radiography Results – Aluminum Symmetric Impact



Density Calculation – Jump Conditions

Impact Velocity

$$u_0 = 1.452 \pm 0.012 \text{ mm}/\mu\text{s}$$

Particle Velocity: $\frac{1}{2} u_0$

$$u_p = 0.726 \pm 0.006 \text{ mm}/\mu\text{s}$$

$P(u_p)$ for 6061-T6 Al

$$P = 1.184 + 140.2u_p + 37.38u_p^2$$

$$P = 12.27 \pm 0.09 \text{ GPa}$$

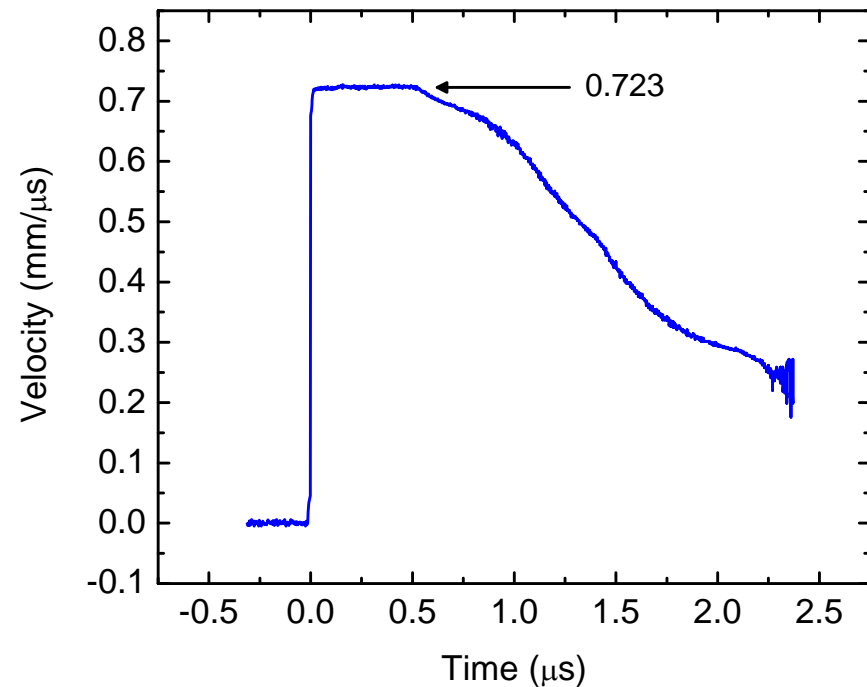
Initial density from immersion

$$\rho_0 = 2.710 \pm 0.003 \text{ g}/\text{cm}^3$$

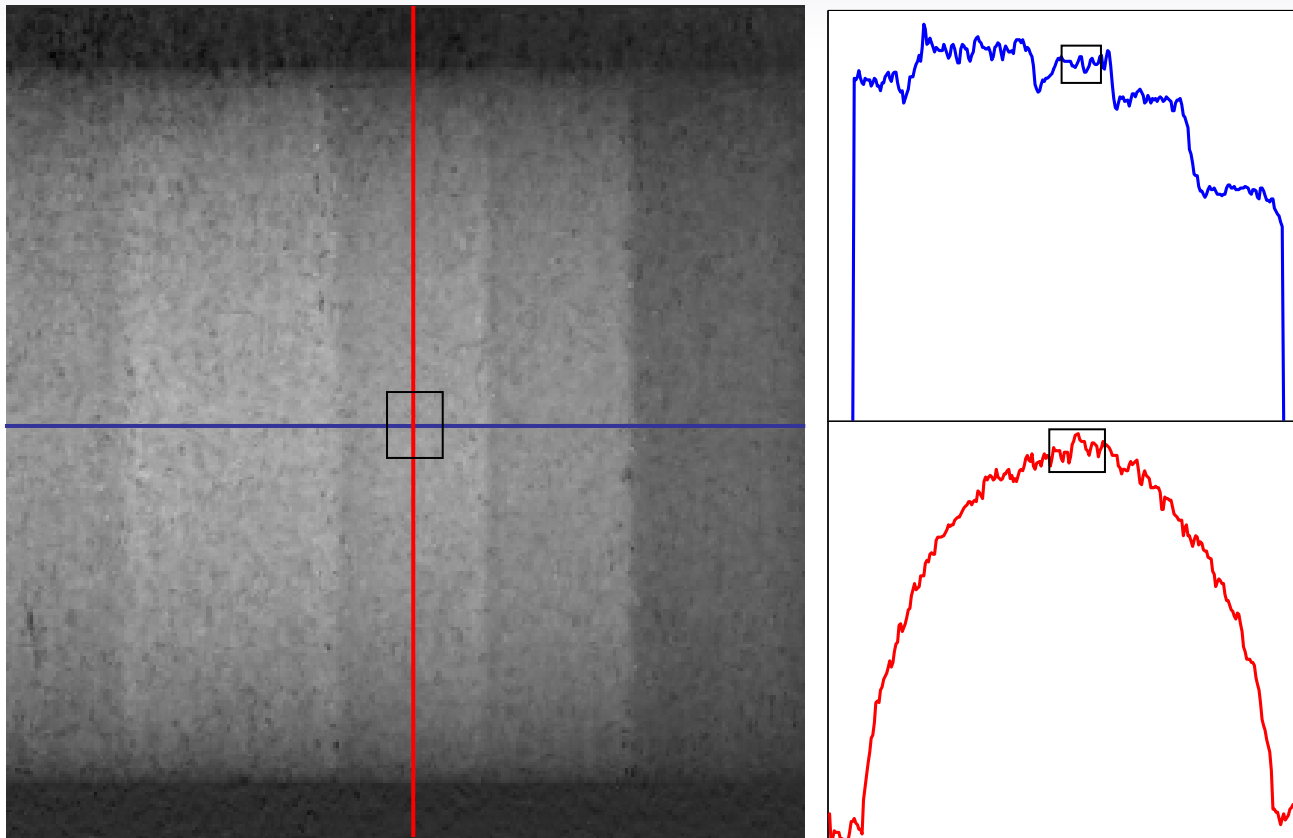
Calculate density from Jump Conditions

$$\rho = \frac{\rho_0 P}{P - \rho_0 u_p^2} \Rightarrow \rho = 3.067 \pm 0.009 \text{ g}/\text{cm}^3 \text{ (0.3\%)}$$

VISAR Record for Shot prad 0198

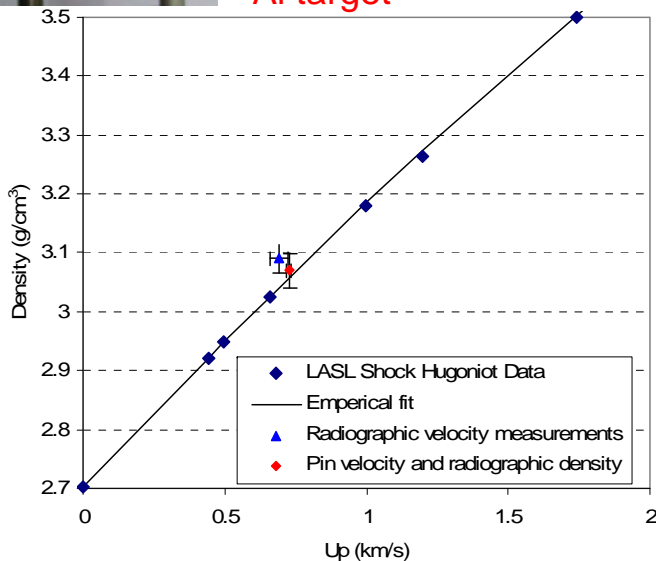
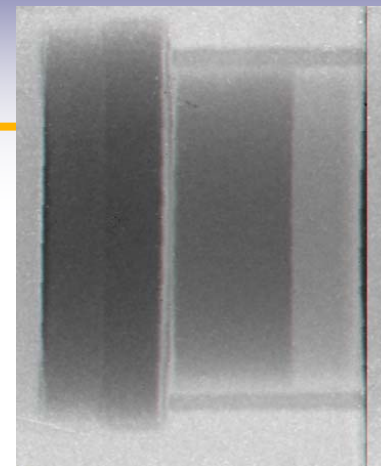
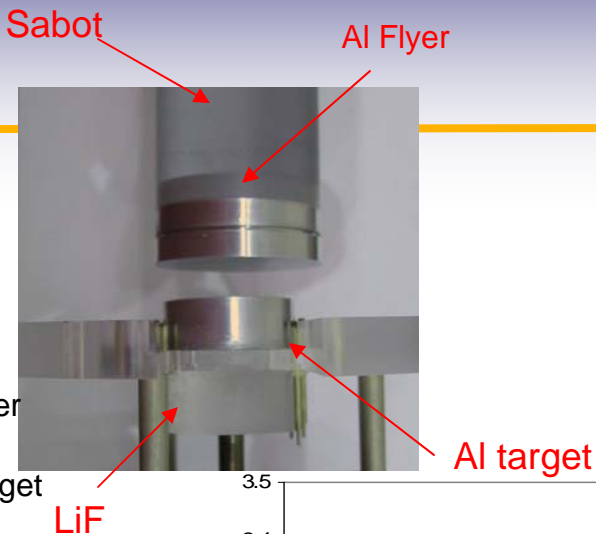
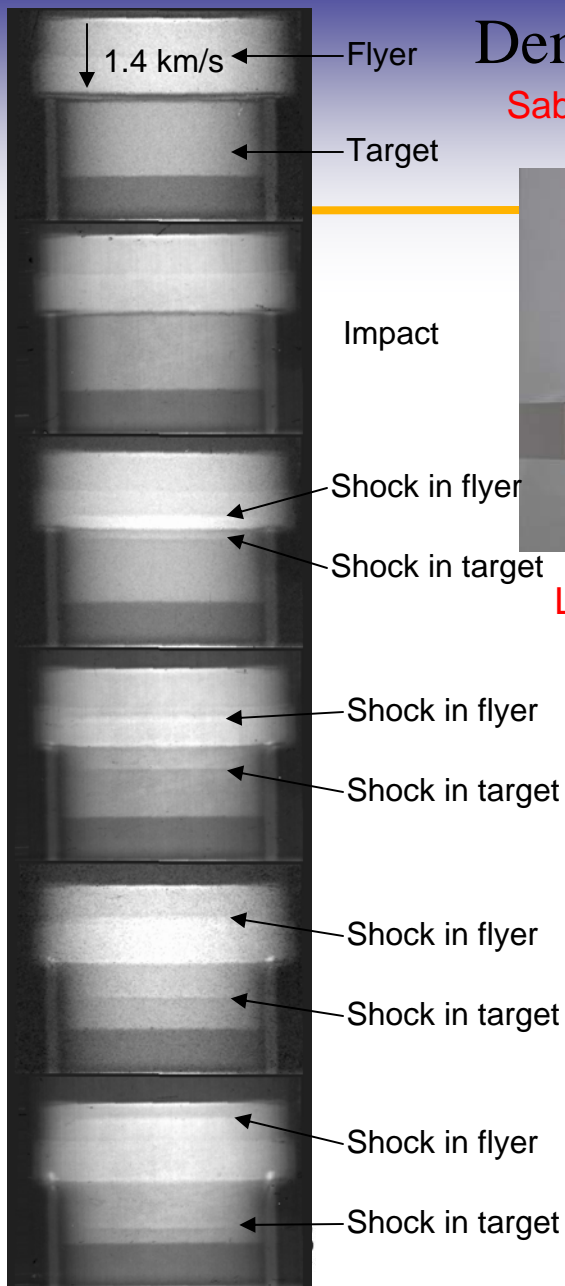


Density Calculation – Abel Corrected Radiograph



Density: $\rho = 3.07 \pm 0.03 \text{ g/cm}^3$ (1.1%)

Demonstration Powder Gun Experiment



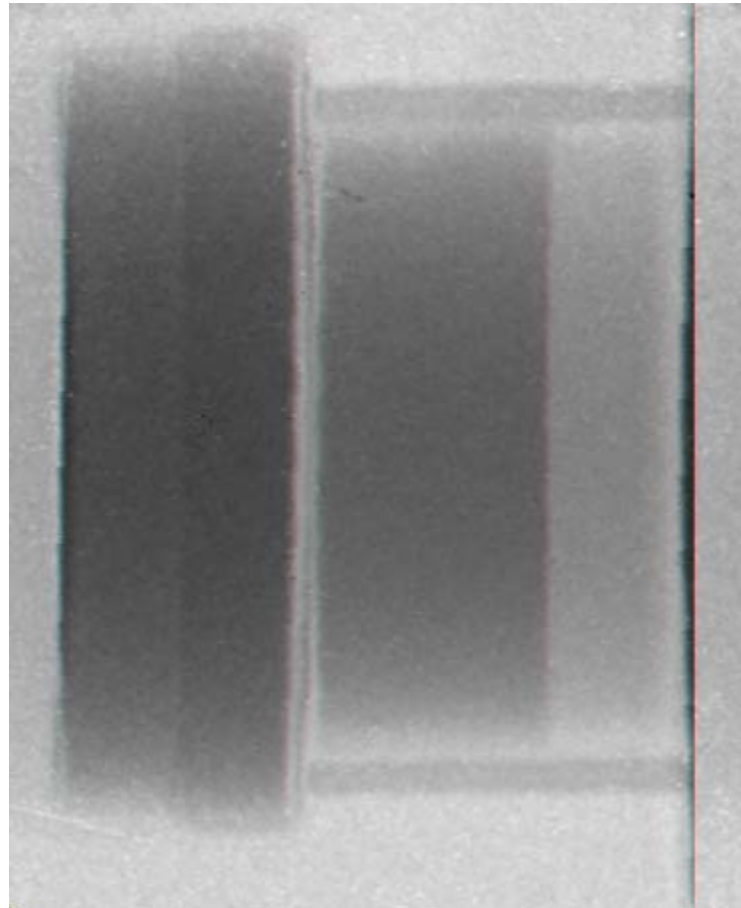
Two methods of measuring a point on shock Hugoniot per dynamic event:

- Radiographic measurement of density behind shock front.
- Simultaneous measurement of particle and shock velocity

Invited Talk : Paulo Rigg, Shock Compression of Condensed Matter, 2007

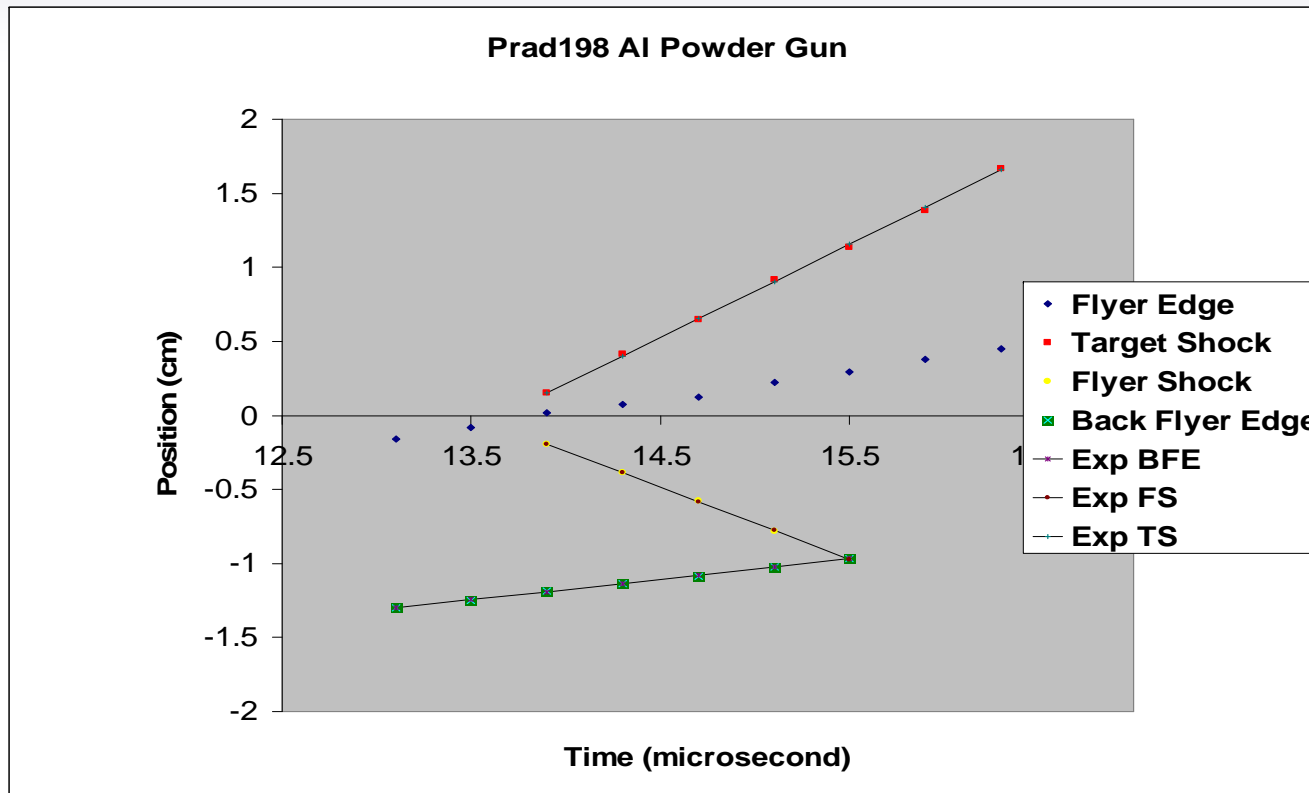
Rigg, Schwartz, et al., Phys. Rev. B, Jun 08, vol. 77, iss. 22 220101

Radiography Results – Aluminum Symmetric Impact



UNCLASSIFIED

Density Calculation – Radiographs



$$f. \text{ Shock: } x_0 + (u_p - u_s)(t - t_0)$$

$$t. \text{ Shock: } x_0 + (u_p + u_s)(t - t_0)$$

$$f. \text{ BEdge: } x_0 + 2u_p(t - t_0) - d$$

$$u_p = .692 \pm 0.06 \text{ mm}/\mu\text{sec}$$

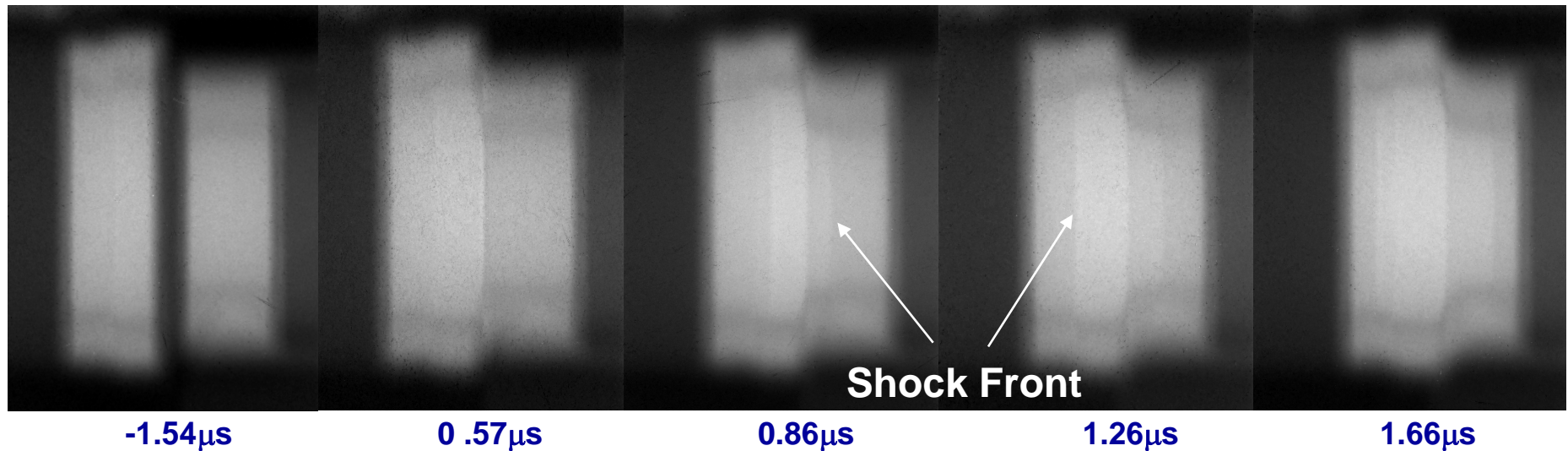
$$u_s = 6.27 \pm 0.04 \text{ mm}/\mu\text{sec}$$

$$\text{Density: } \rho = 3.04 \pm 0.024 \text{ g/cm}^3$$

$$\text{Ex Density: } \rho = 3.067 \pm 0.009 \text{ g/cm}^3$$

Results from Copper Symmetric Impact Experiment

Flyer velocity \longrightarrow



- Significant distortion present due to higher density of copper
- Distortions do not affect measurement

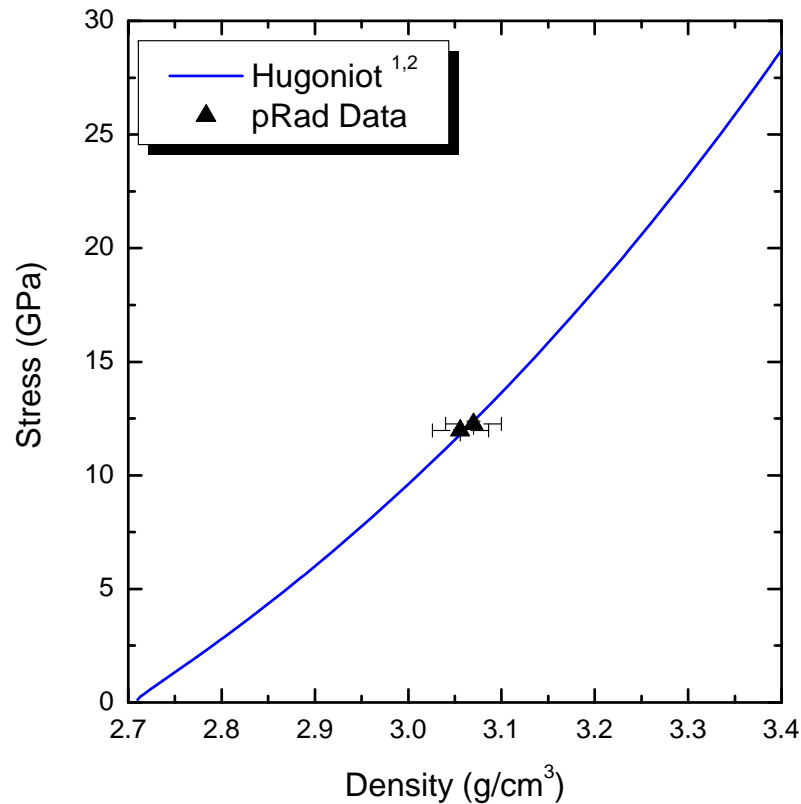
Experiment Summary

Experiment	Impactor/ Sample	Impactor Velocity (km/s)	Peak Stress (GPa)	Initial Density (g/cm ³)	Calculated Density (g/cm ³)	Measured Density (g/cm ³)	Agreement
1	Al 6061-T6	1.452 (0.012)	12.27 (0.11)	2.710 (0.003)	3.067 (0.005)	3.07 (0.03)	0.1%
2	Al 6061-T6	1.422 (0.002)	11.98 (0.03)	2.710 (0.003)	3.060 (0.004)	3.056 (0.03)	0.1%
3	OFHC Cu	1.30 (0.04)	28.59 (0.91)	8.928 (0.003)	10.30 (0.05)	10.28 (0.10)	0.2%
4	OFHC Cu	1.249 (0.002)	27.16 (0.06)	8.928 (0.003)	10.241 (0.006)	10.28 (0.10)	0.4%

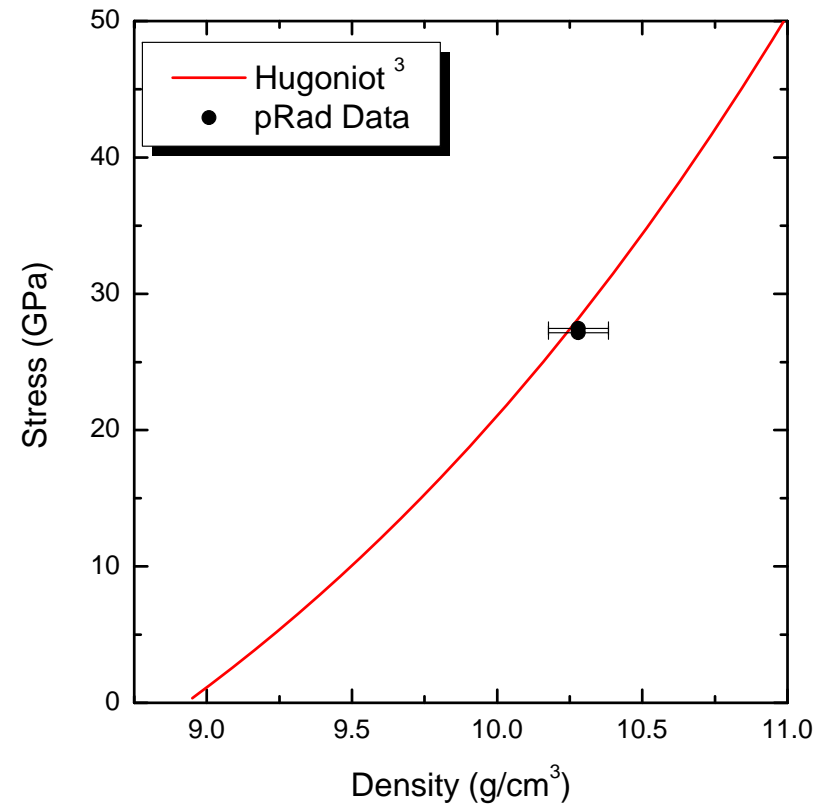
- Agreement between measured and calculated values better than 0.5% for all experiments

Measured Density Values Lie on Hugoniot

6061-T6 Aluminum



OFHC Copper



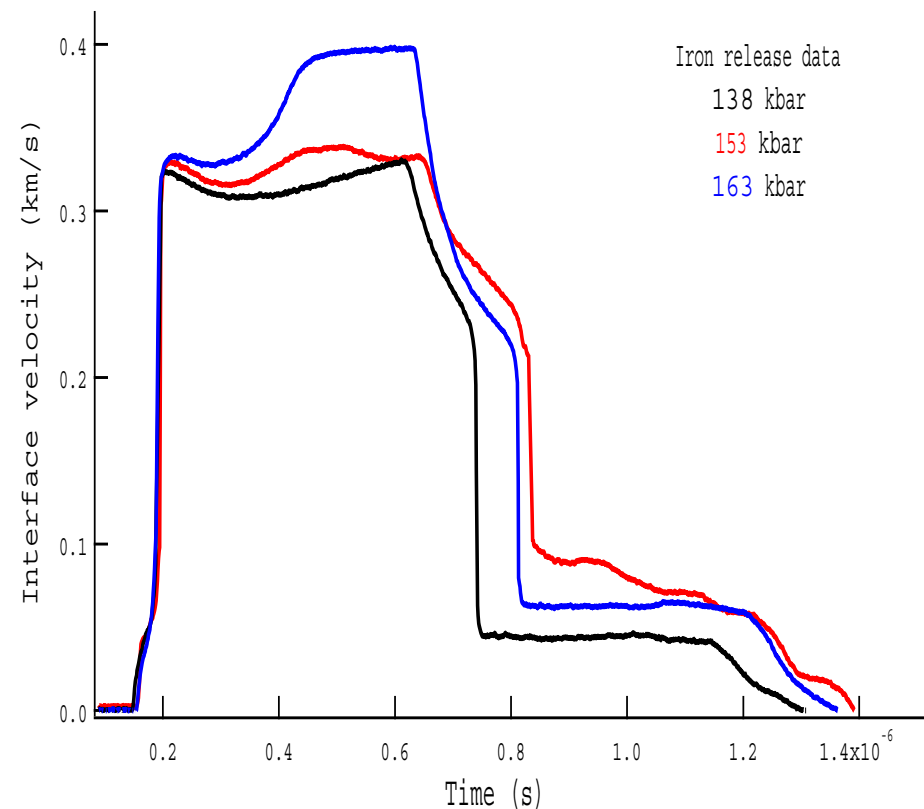
(1) C. D. Lundergan and W. Herrmann, J. Appl. Phys. **34**, 2046 (1963).

(2) W. M. Isbell and D. R. Christman, Tech. Rep. MSL-69-60, General Motors (1970).

(3) R. G. McQueen, S. P. Marsh, J. W. Taylor, et. al., *High Velocity Impact Phenomena* (Academic Press, New York, 1970).

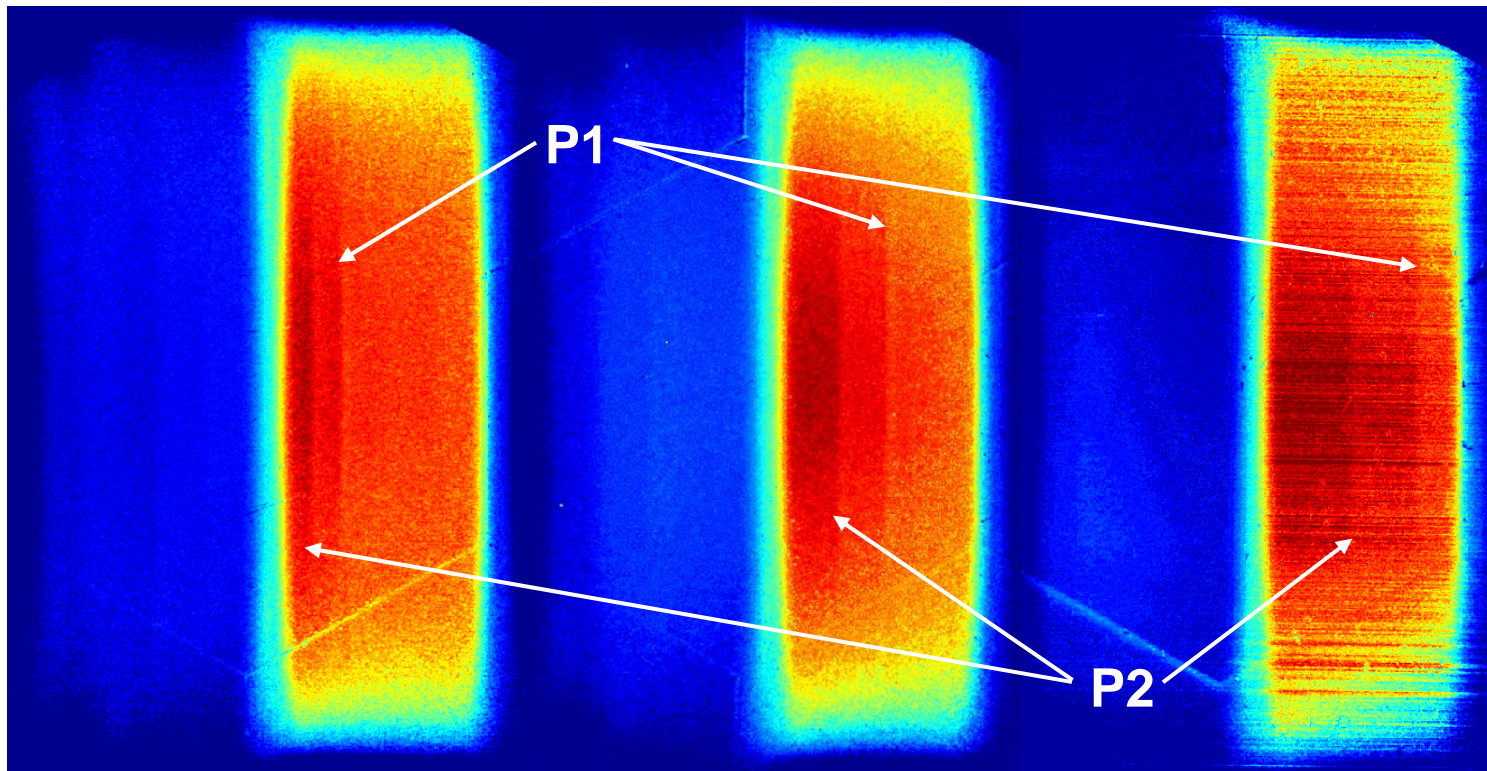
Phase Transition Studies: Iron

- α to ϵ transition observed in Fe at ~ 13 GPa
- Transition is relatively insensitive to purity
- Reverse transition clearly observed as evidence by rarefaction shock

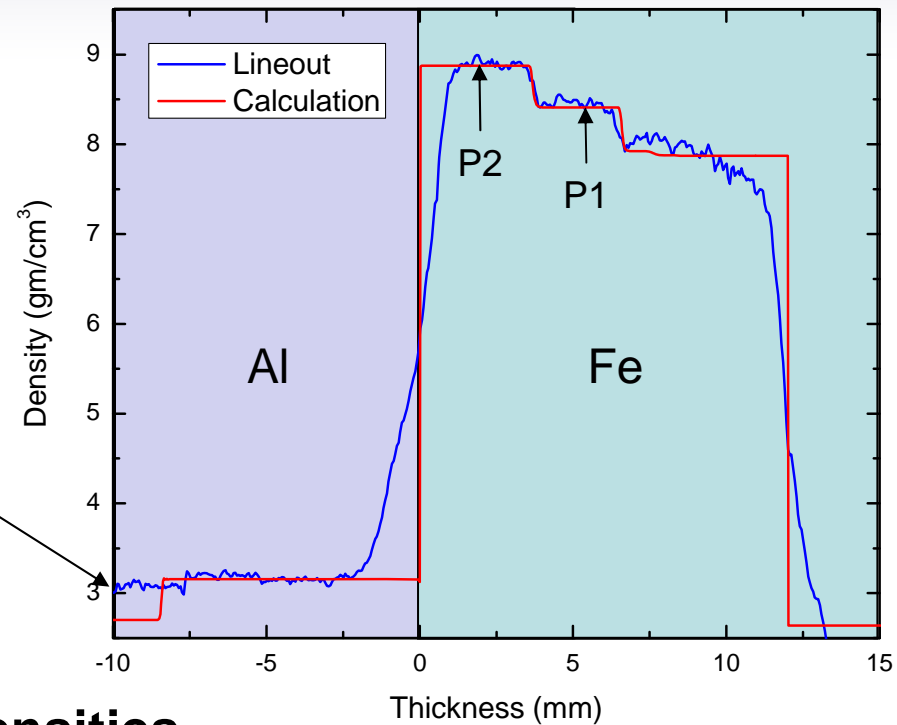
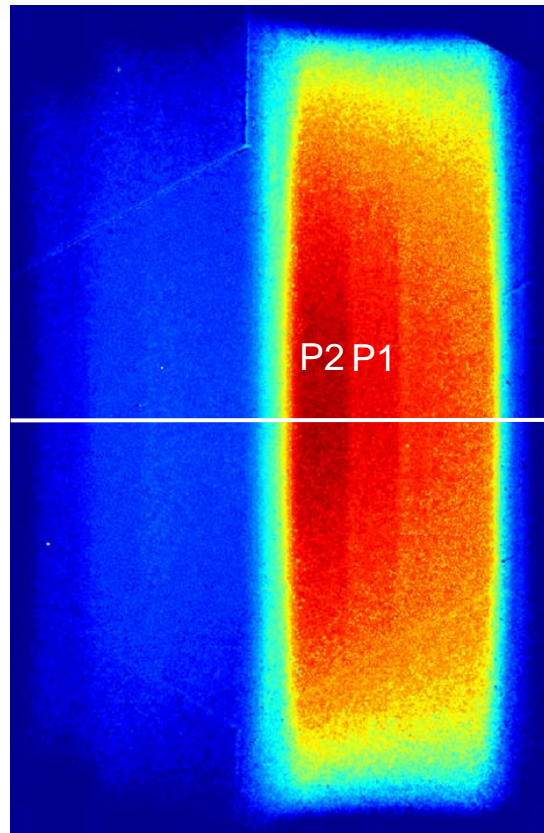


Two-wave structure observed in Iron

- Aluminum impacting Iron backed by Sapphire @ 1.45 km/s -> 175 kbar in Fe
- 3X pRad Magnifier used to enhance contrast and sharpness



Measured and Calculated Densities - Iron



Densities

State	Measure	Calculat	Agreem
P1	8.346	8.342	<0.1%
P2	8.854	8.846	0.1%

UNCLASSIFIED

Conclusions

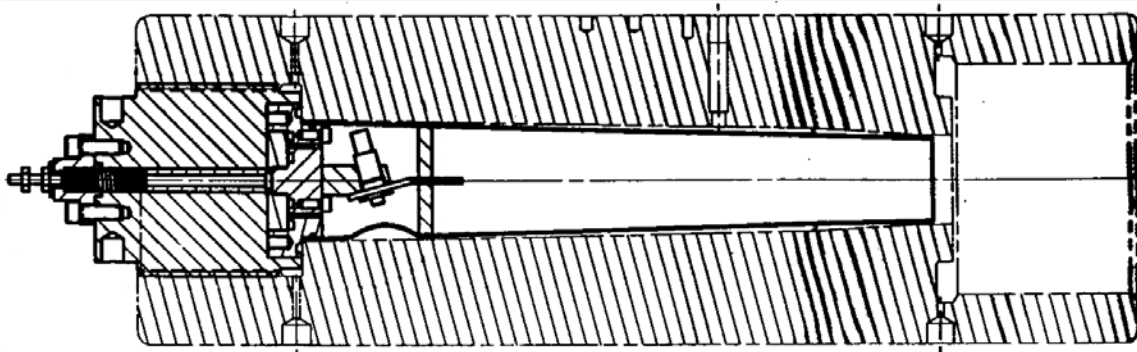
- Successfully coupled proton radiography with plate impact experiments
- Direct density measurements obtained in shocked aluminum, copper and iron with $\sim 1\%$ precision
- **Agreement with calculated values better than 0.5%!**
- Large difference in initial density between Cu and Al shows wide applicability to other materials
- Future work: Cerium to examine solid-solid and solid-liquid phase transitions...

40mm Launcher Design Details

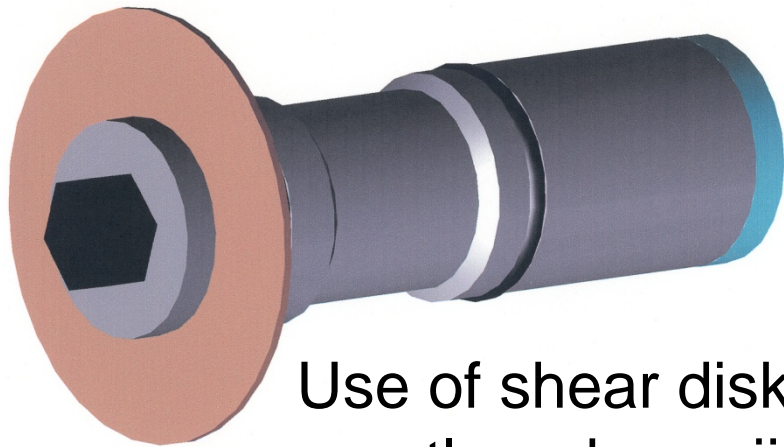
- Completely enclosed system designed to couple plate impact experiments with Proton Radiography
- Uses gun powder and an SE-1 detonator to launch projectiles up to 2 km/s (600 kbar in copper using Ta flyer)
- Produces planar impact on samples up to 40mm in diameter
- Free floating barrel design and shock absorber system minimize recoil load transferred to Proton beam tubes



Synchronization



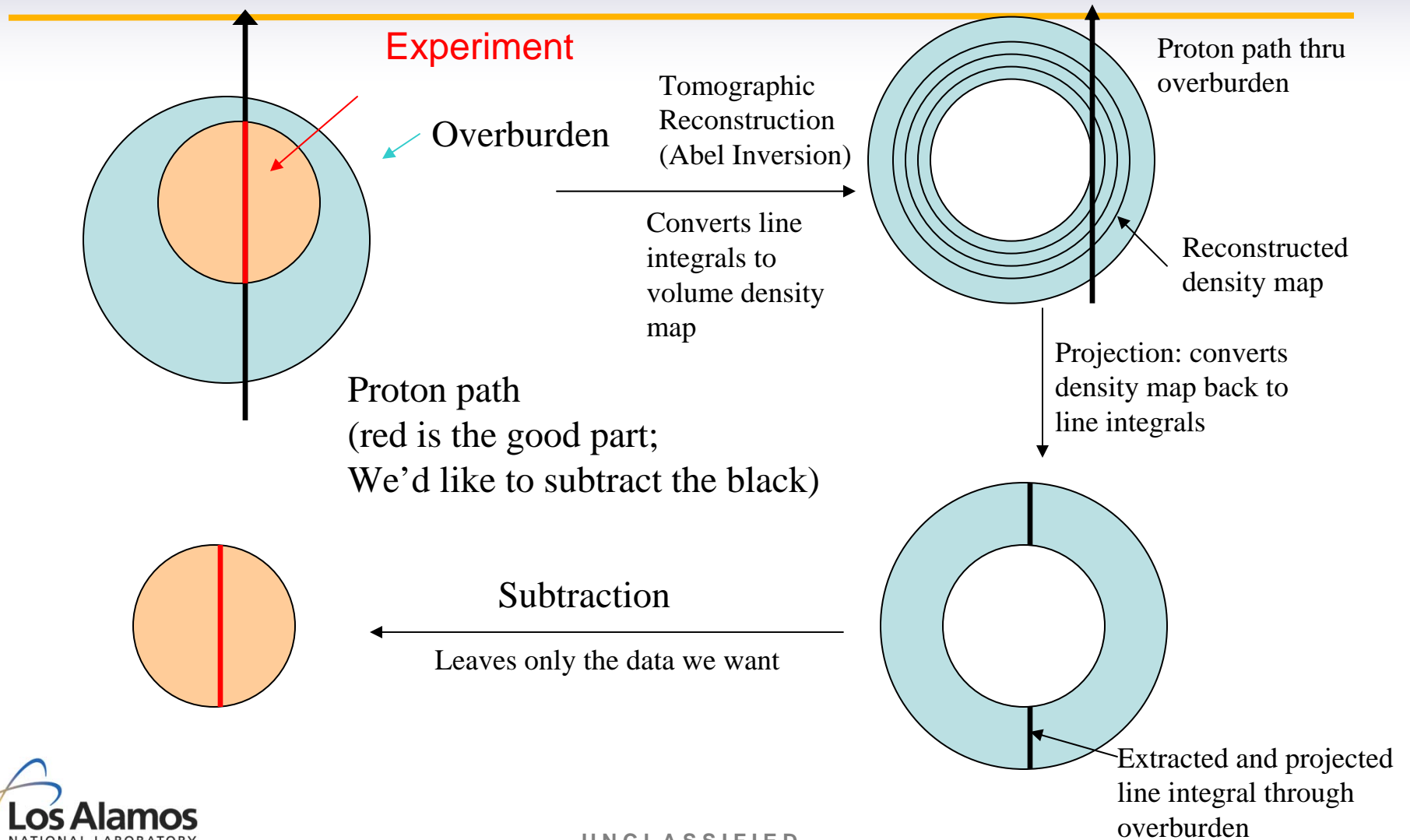
Det fired system:
Beamline initiates gun



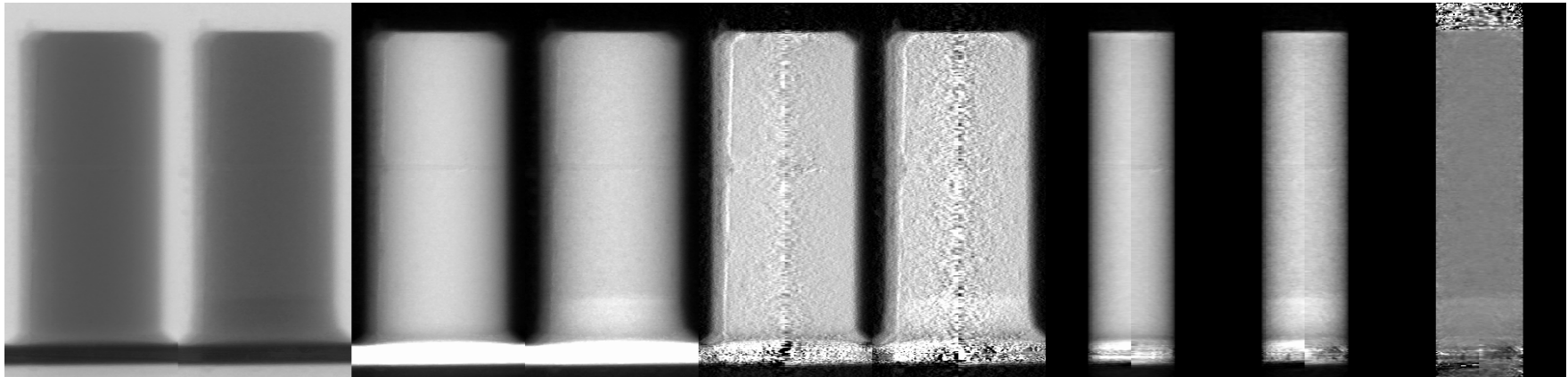
Use of shear disk
greatly reduces jitter



Tomographic reconstruction and subtraction of overburden



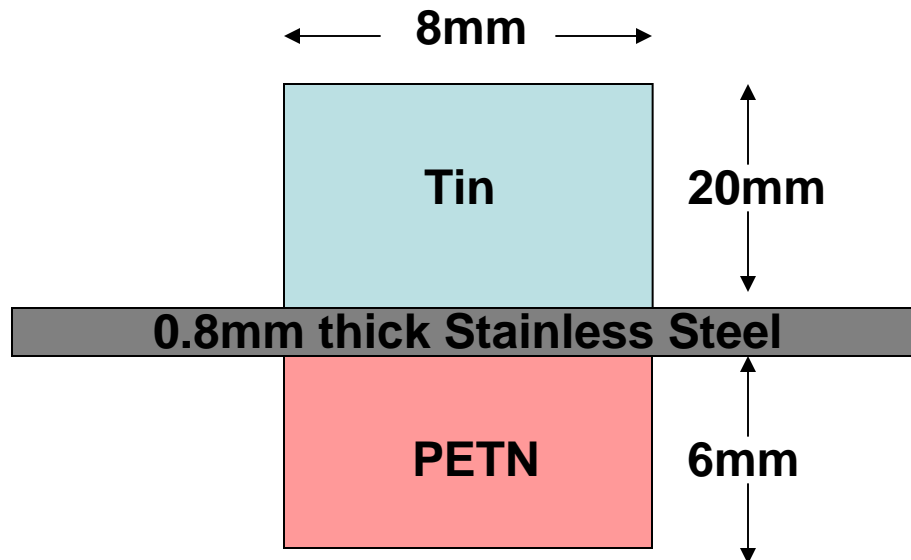
Trimmed density reconstruction



Technique that subtracts overburden and release effects from areal density radiographs

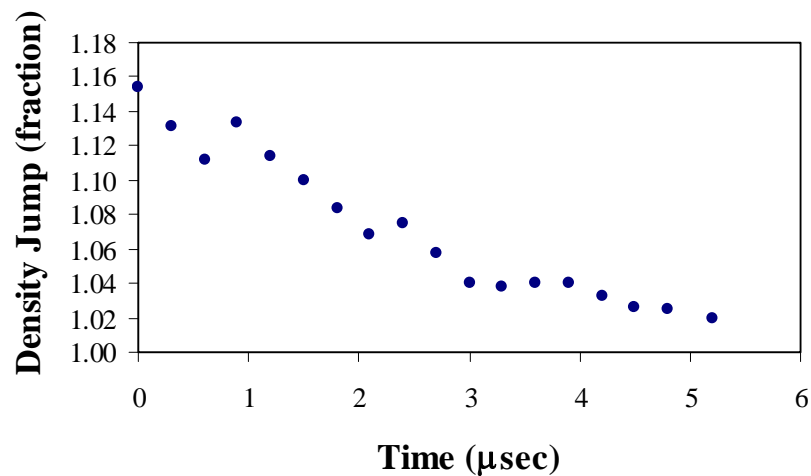
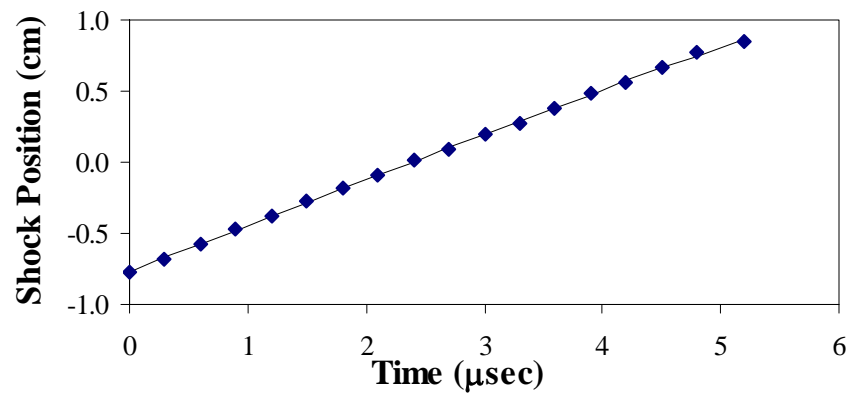
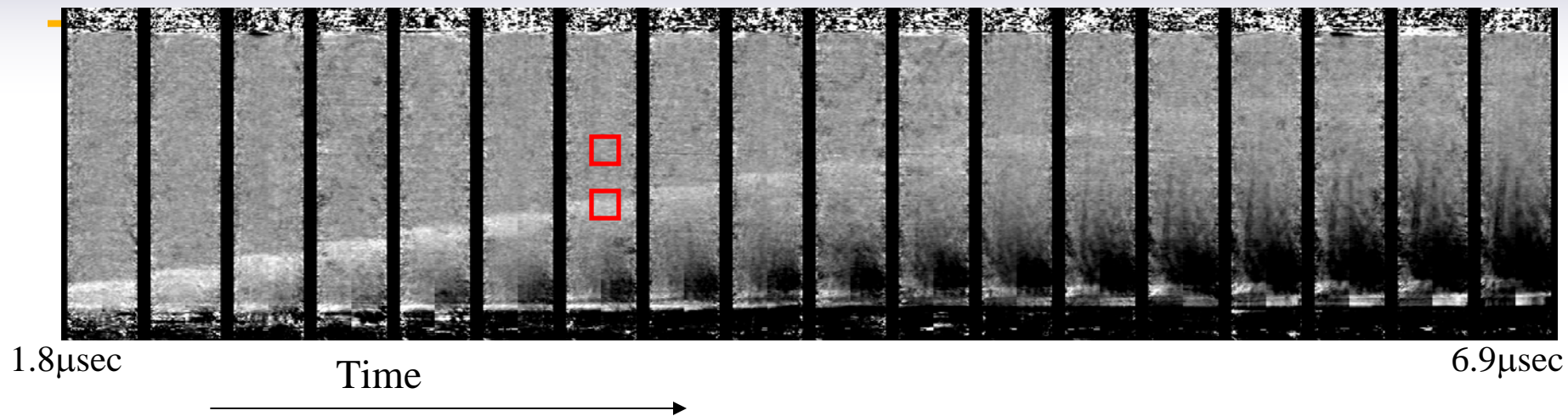
Taylor Wave-Driven Tin

- Explosive-driven “Taylor Wave” shock
- Multiple pressures, decaying over time
- Stainless steel membrane



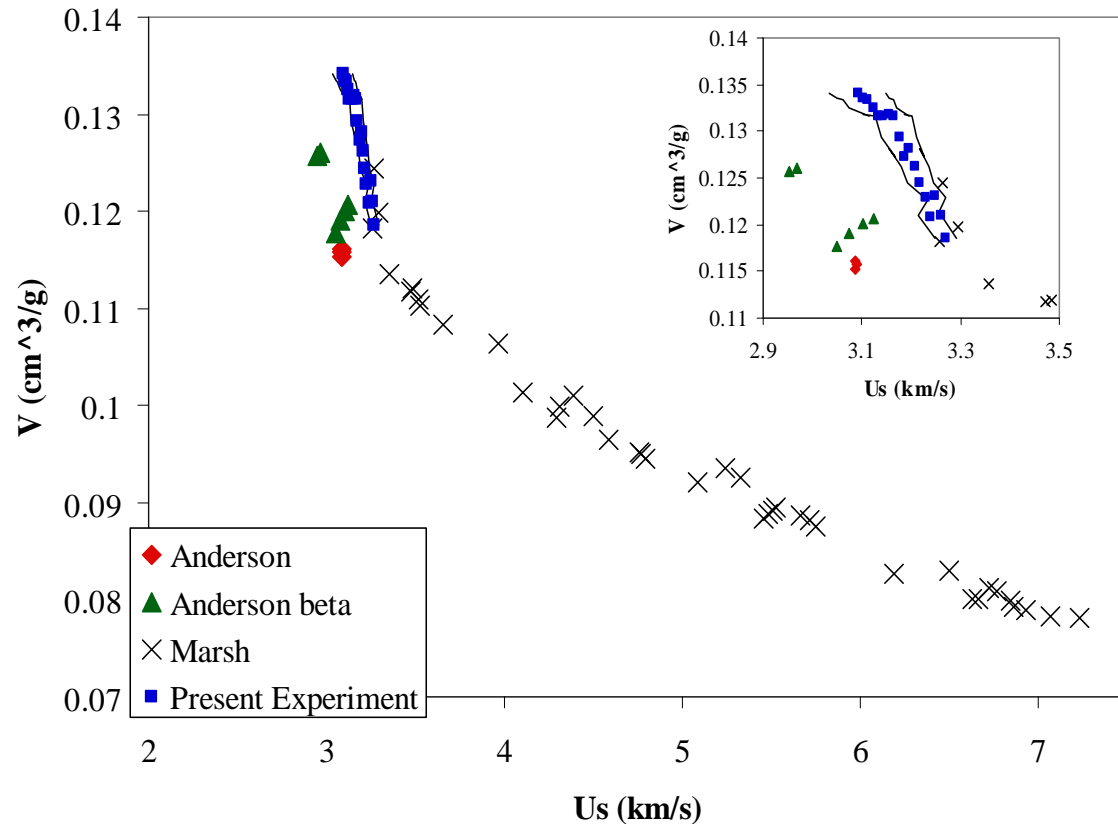
Dynamic / Static transmission radiographs

Position and Density Measurements



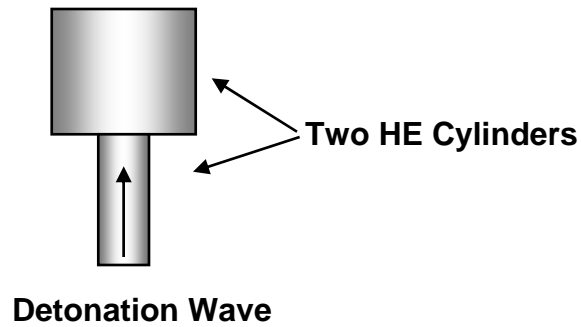
Single experiment, Multiple Measurements

- Single experiment measures many Hugoniot points
- Agreement with LASL Hugoniot data
- Hugoniot points measured from peak shock velocity down to nearly sound velocity

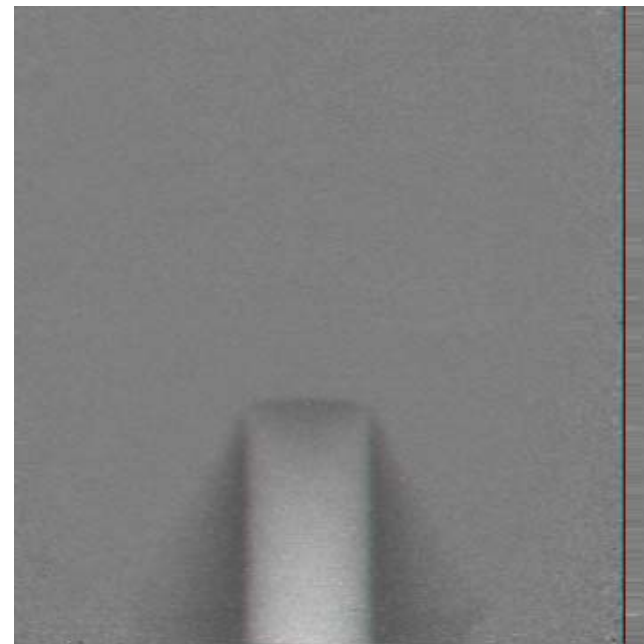


PBX 9502 First Corner Turner Experiment

Campbell -Cox experiment on corner turning in Insensitive HE



Prad0043



PBX9502 corner turning experiment



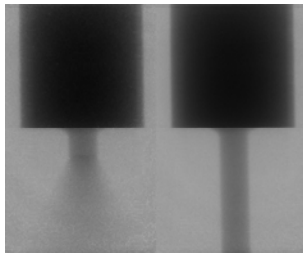
Volume densities

Prad0067
18 mm donor

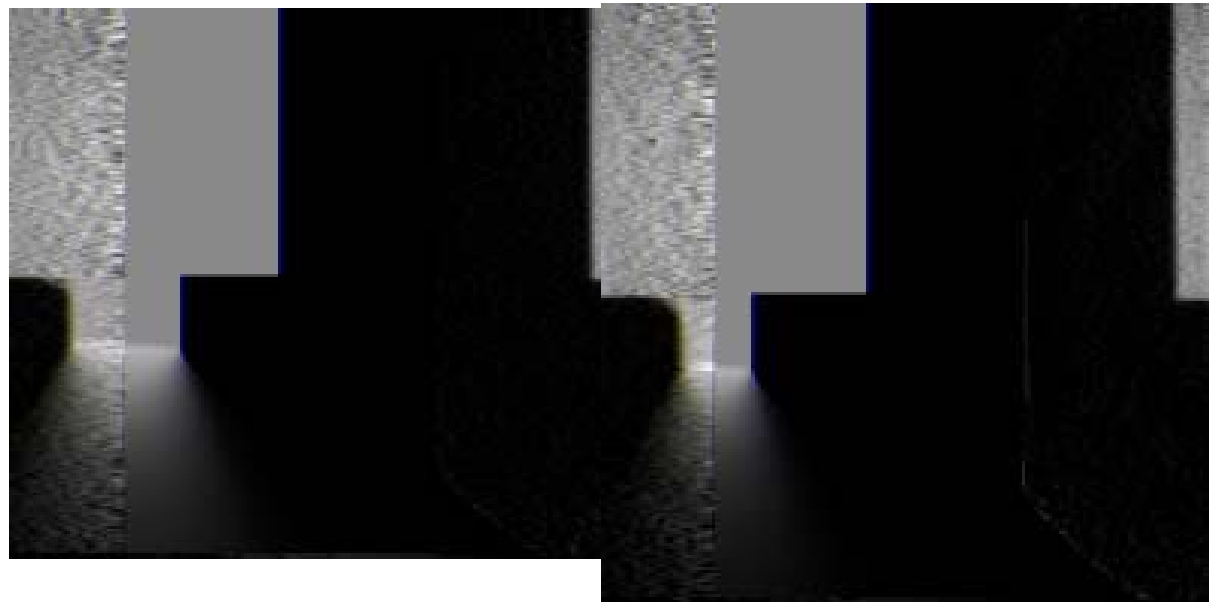
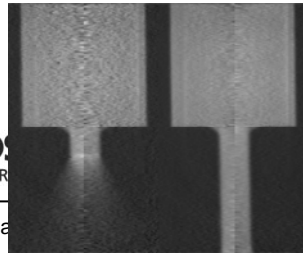
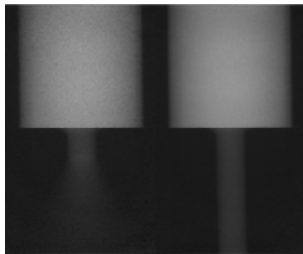
Prad0068
12 mm donor

Dynamic Static

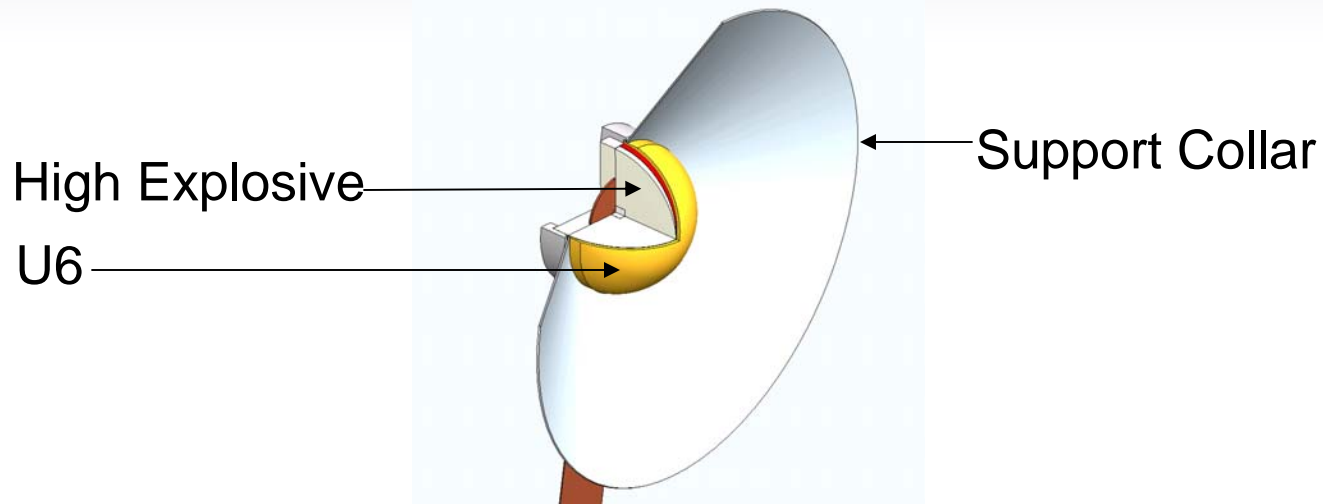
Transmission



Areal density

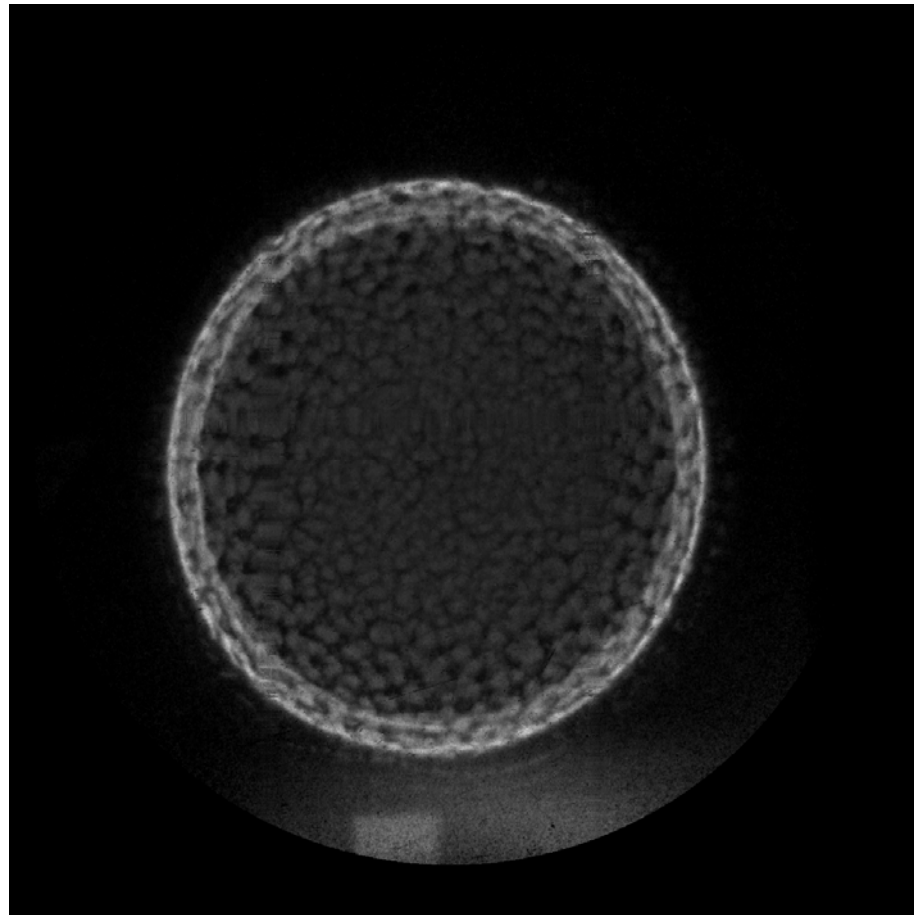
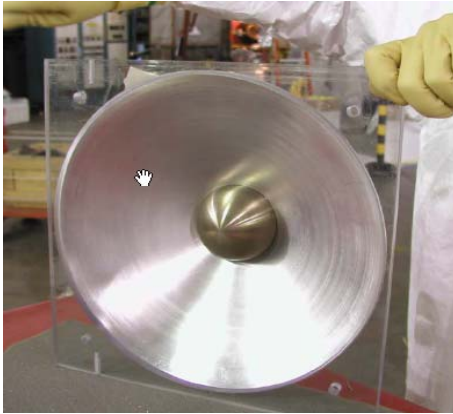


Proton Radiograph Captures Fragmentation over Time

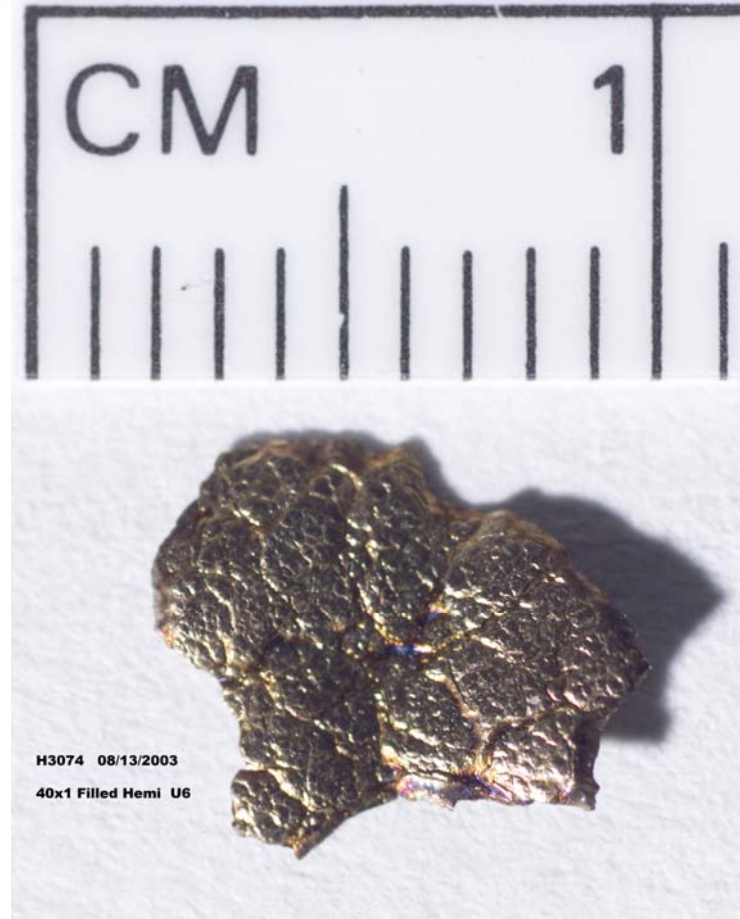


- Hemisphere of U6 is explosively expanded.
- Proton radiograph captures fragmentation over time
- Percent open/closed area is calculated from 100 random locations
- Support vector machine is used to categorize entire data set

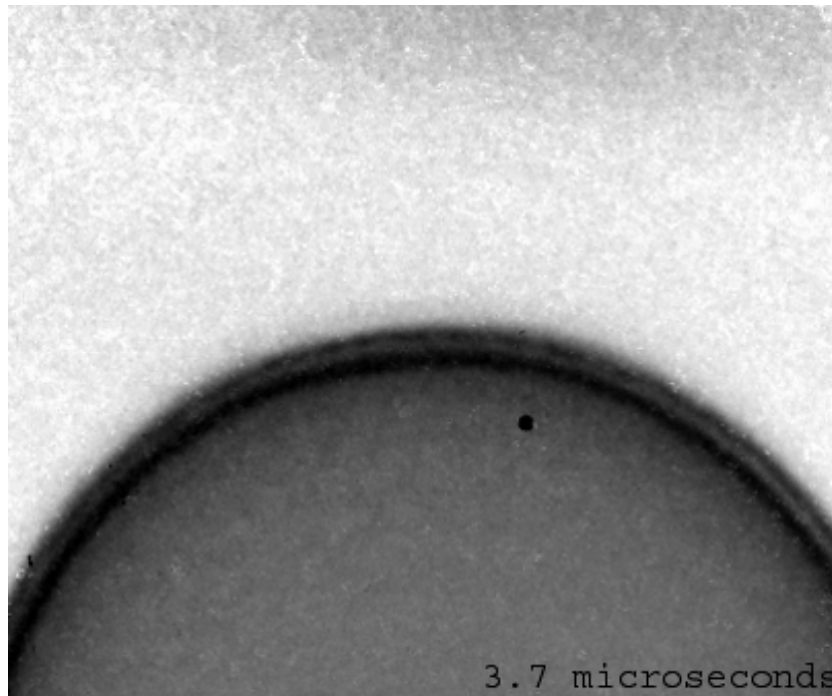
Shear Band Failure in U6Nb



Fragments Can be Recovered through “Soft Catch”



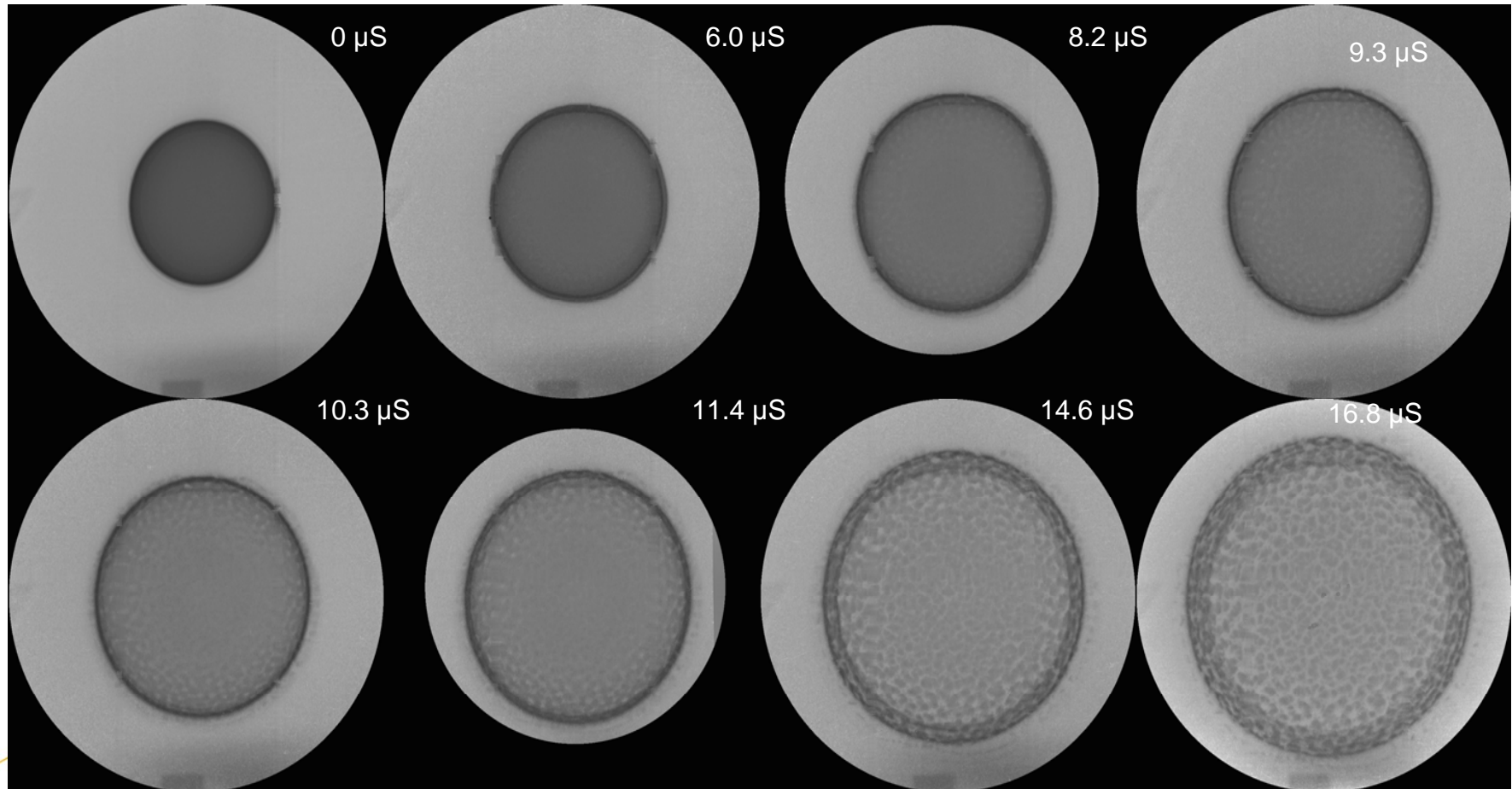
Shear Localization and Breakup



Frame 0:	0 μs	pre-Shot Static
Frame 1:	3.7 μs	hint of localization
Frame 2:	5.9 μs	clear localized thinning
Frame 3:	7.0 μs	continued thinning
Frame 4:	8.0 μs	localization points begin to connect
Frame 5:	11.4 μs	continued fragmentation
Frame 6:	14.6 μs	fragments formed
Frame 7:	16.8 μs	ballistic motion

UNCLASSIFIED

Shear Band Failure in U6Nb



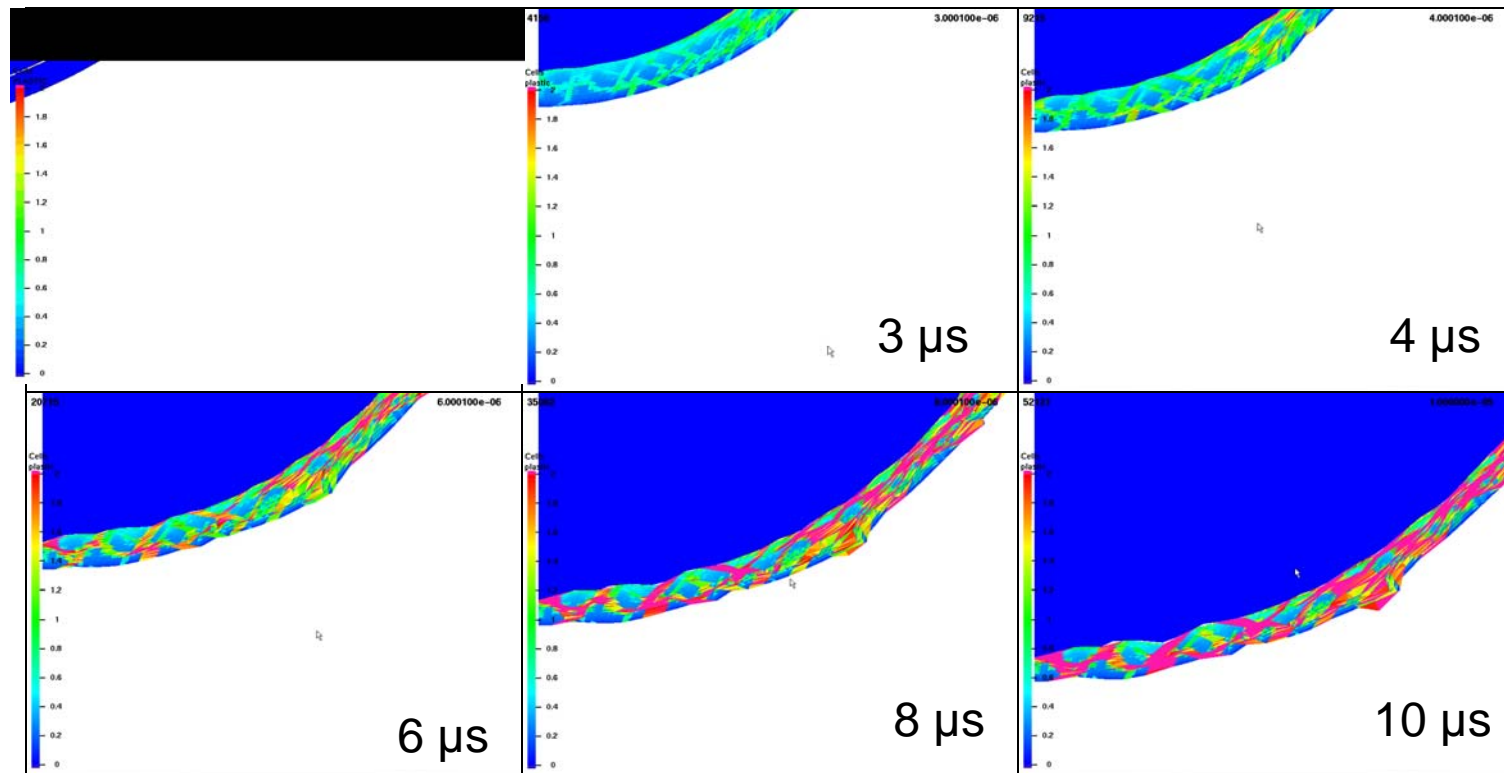
NATIONAL LABORATORY
EST. 1943

UNCLASSIFIED

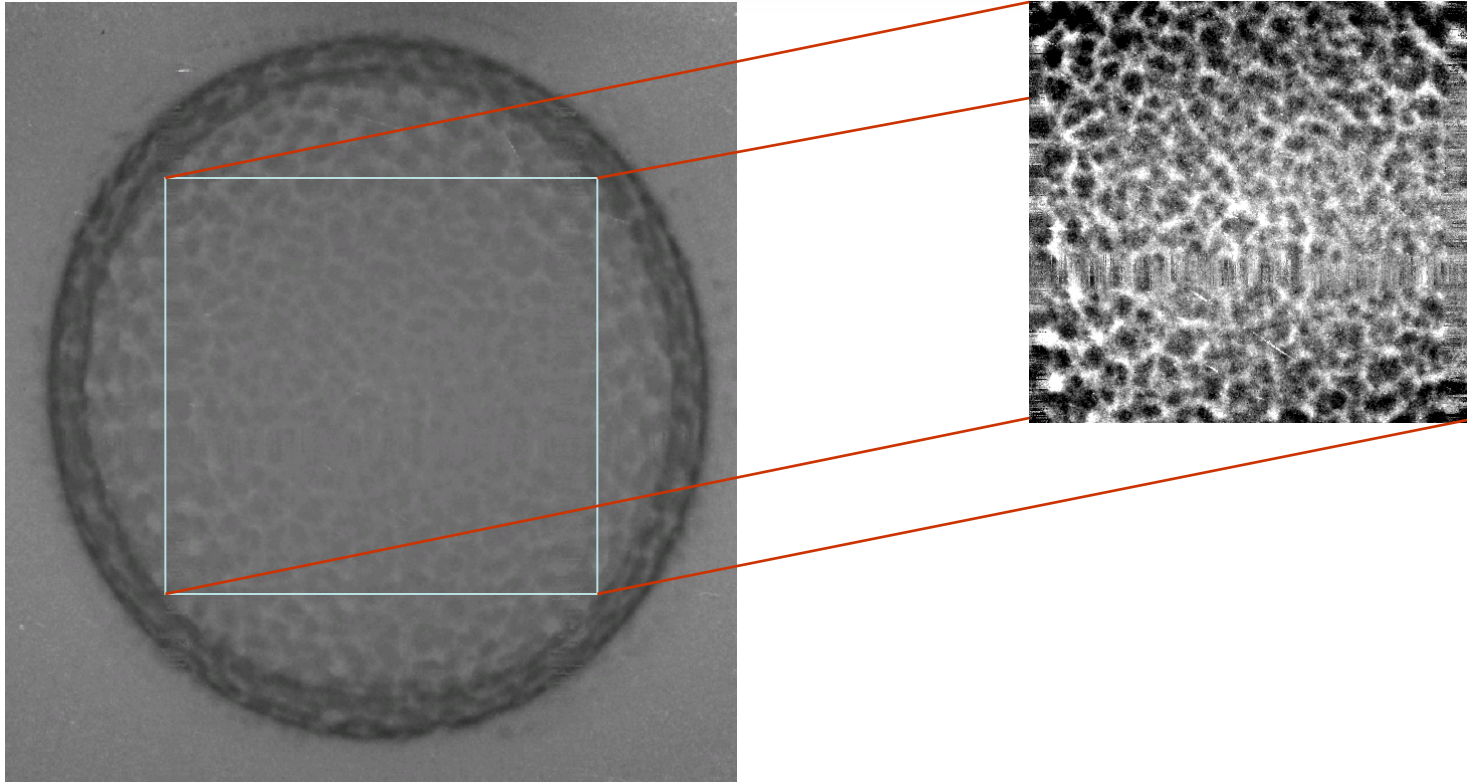
Operated by the Los Alamos National Security, LLC for the DOE/NNSA



Shear Band Failure in U6Nb



We Estimate Percent Open Area from 100 Random Locations

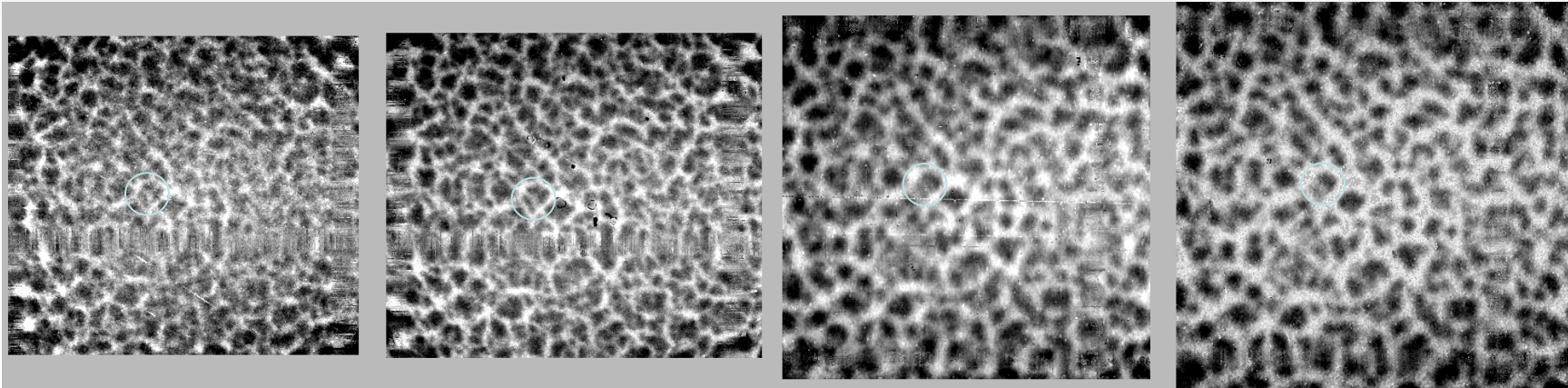
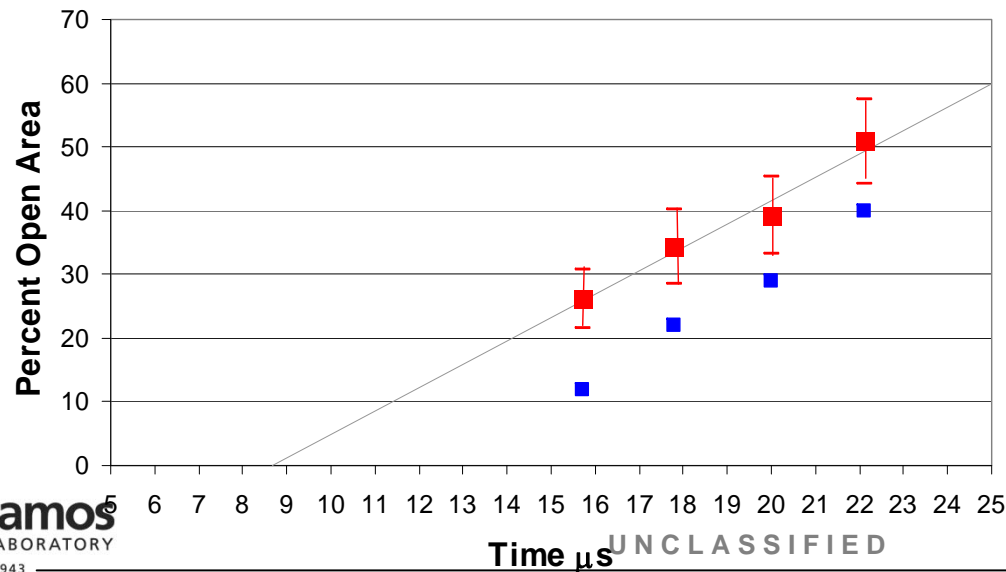


10mnstfprad0161Shot2.tif

- 100 random points are thrown at the data set
- Metal/Not-metal determined at each point by eye
- Tedious, but very effective

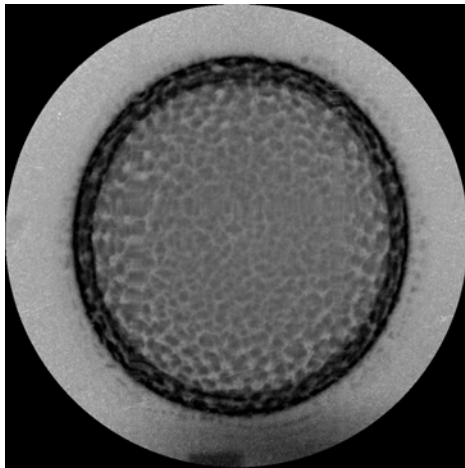
UNCLASSIFIED

This Procedure is Repeated over Four pRad Time Steps by 15 Individuals

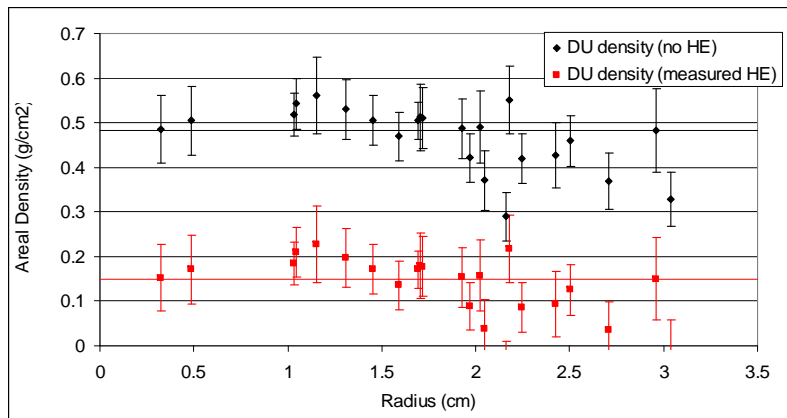
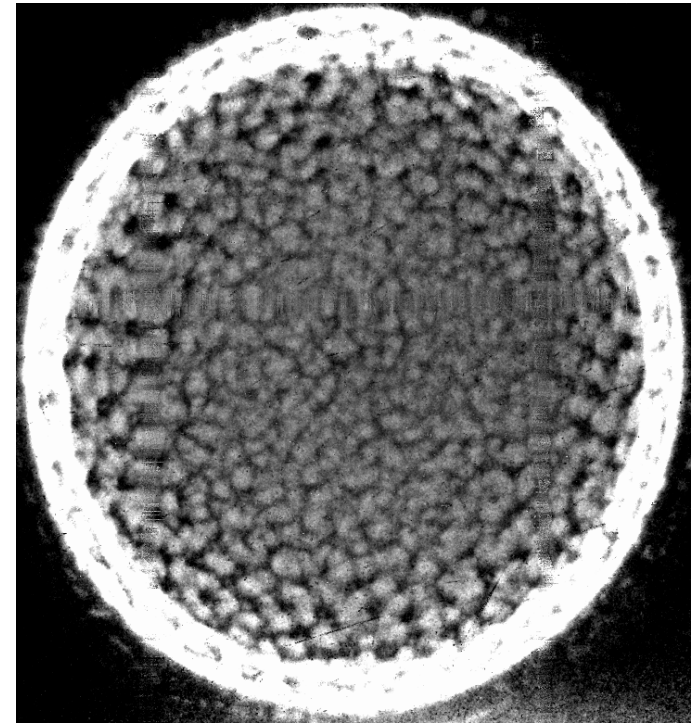
15.7 μ s 26% open17.8 μ s 34% open20.0 μ s 39% open22.1 μ s 51% open

■ Average of 15 observers ± 1 std
■ Initial untrained observer

Shear Band Failure in U6Nb



- Assume no HE products to give max DU density.
- Assume flat measured HE products to calculate min DU density.
- Results bracket density in cracks.



pRad has allowed the mechanism for high explosive cookoff to be better understood

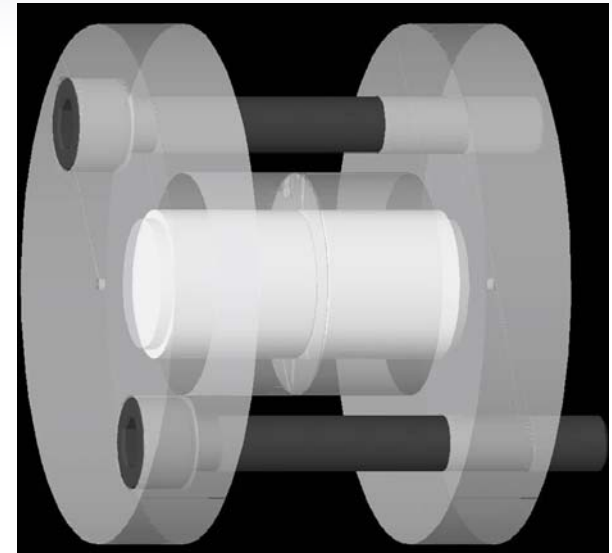
-

USS Enterprise-1969
Aircraft accident and subsequent cook off explosions
27 killed 314 injured



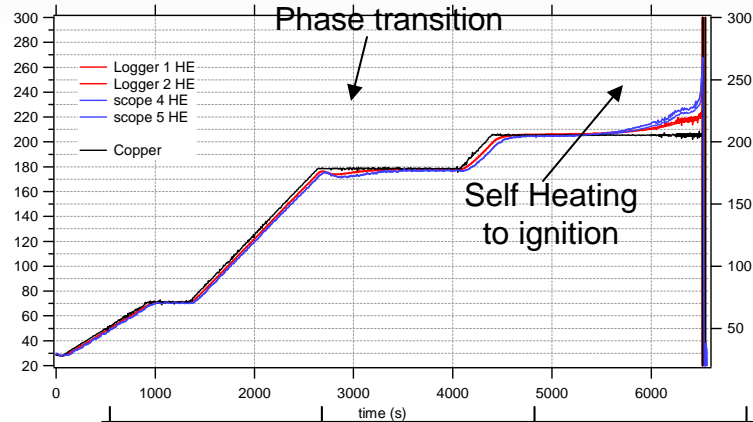
Cookoff Experiments

- Thermal ignition experiment studying properties of PBX-9501 for the surety program
- Study pre-ignition material density changes
- Study post-ignition reaction propagation
- Material drive mechanisms
- Previous measurements have been performed with optical diagnostics
- Proton radiography provides information on:
 - Pre-ignition density variations of HE
 - Ignition propagation
 - Encasing material drive

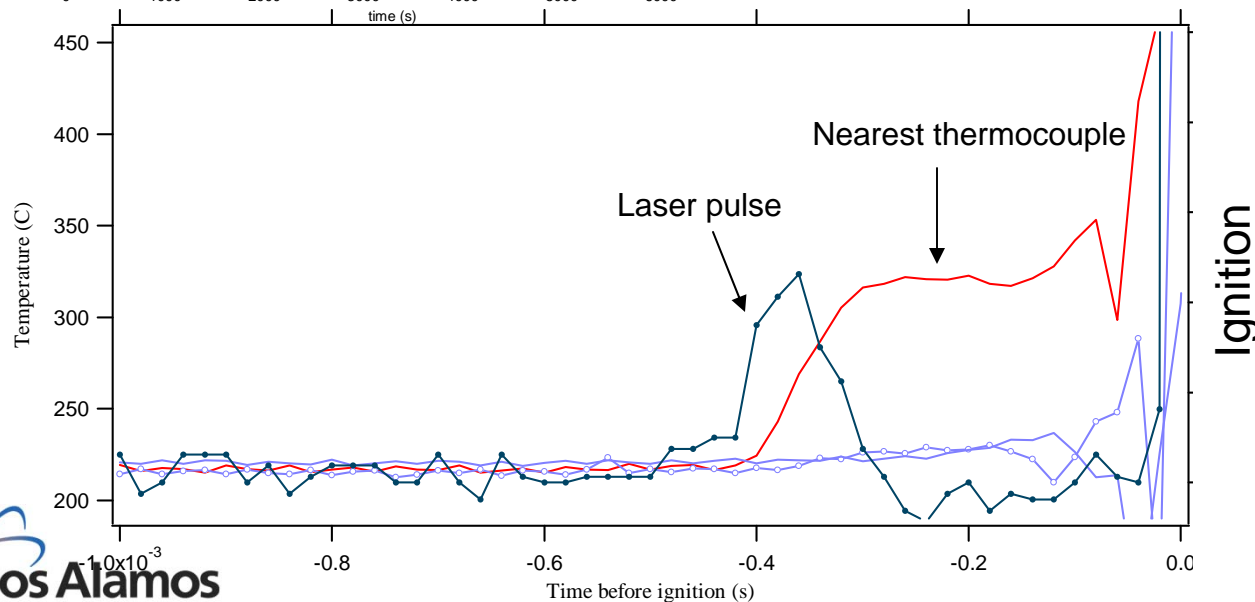


Laser Synchronization

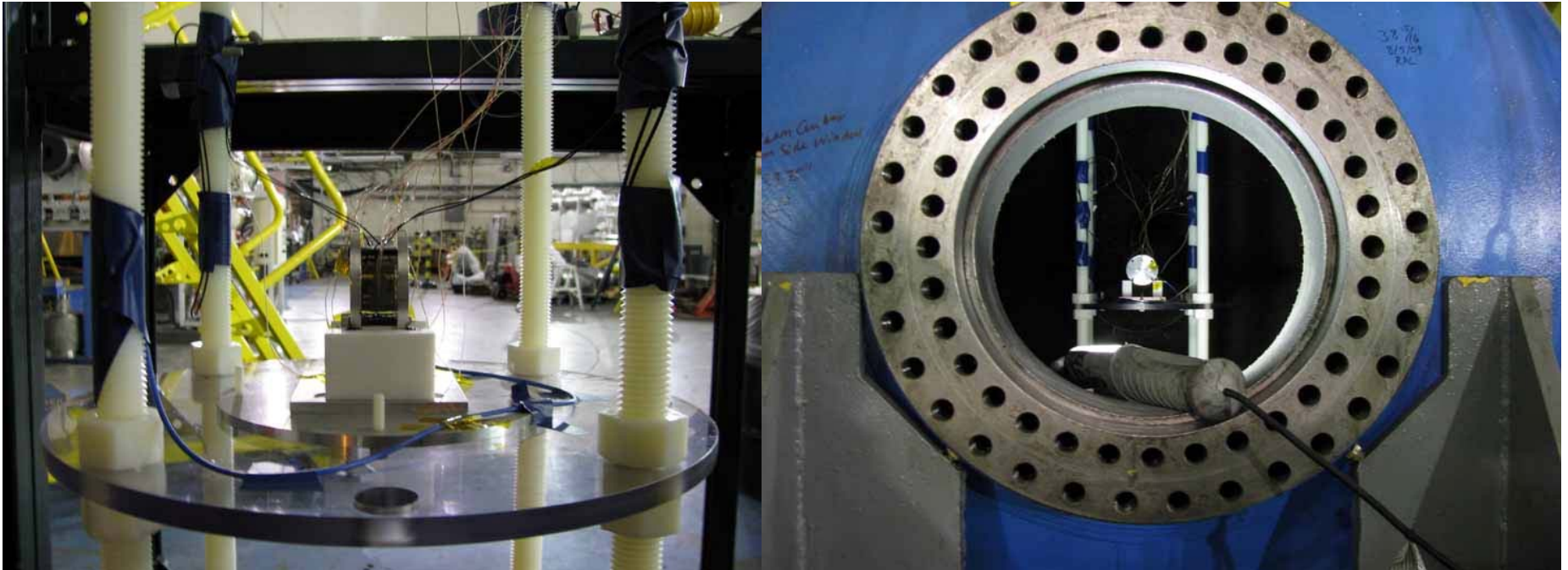
Temperature Ramp



- Human synchronization to within a minute.
- Laser induced ignition synchronization of event and beam to $\sim 100 \mu\text{S}$.



Cookoff Shot Setup

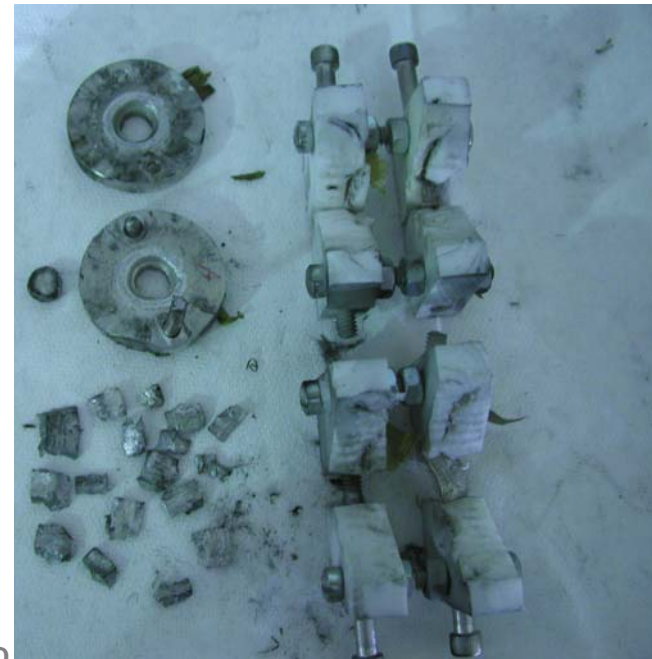
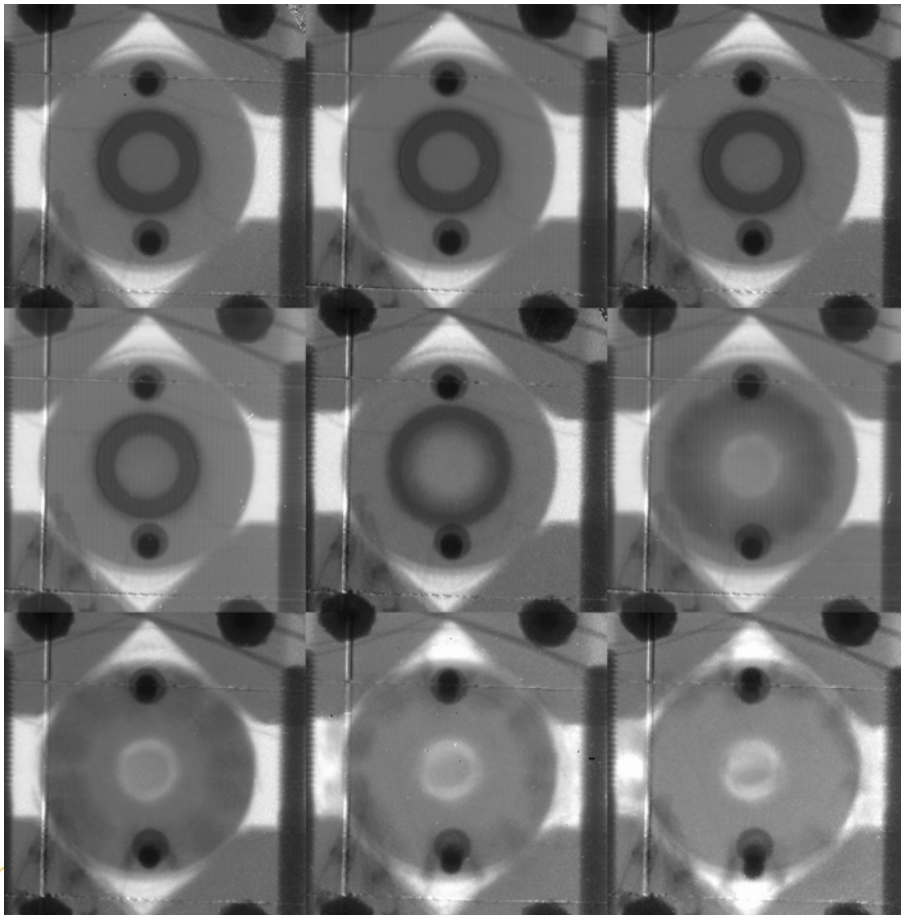
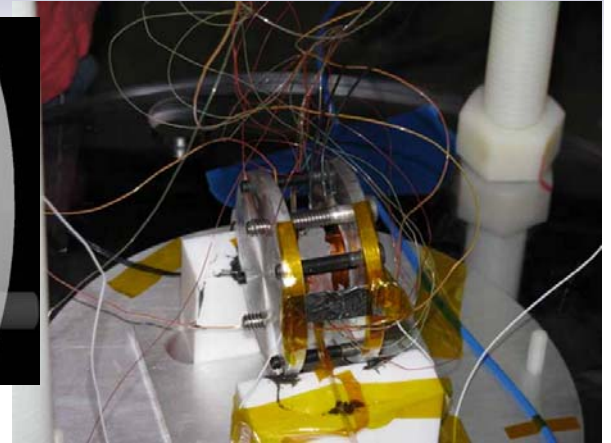
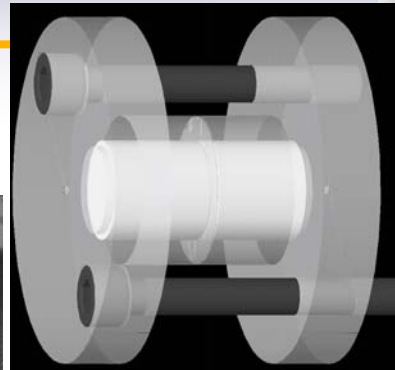
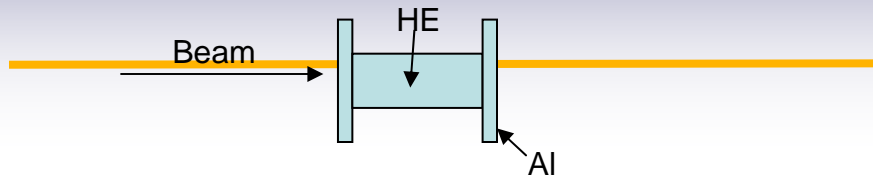


Fiber optic cable attached for laser ignition

Thermocouples embedded for temperature reading

UNCLASSIFIED

Successful Synchronization



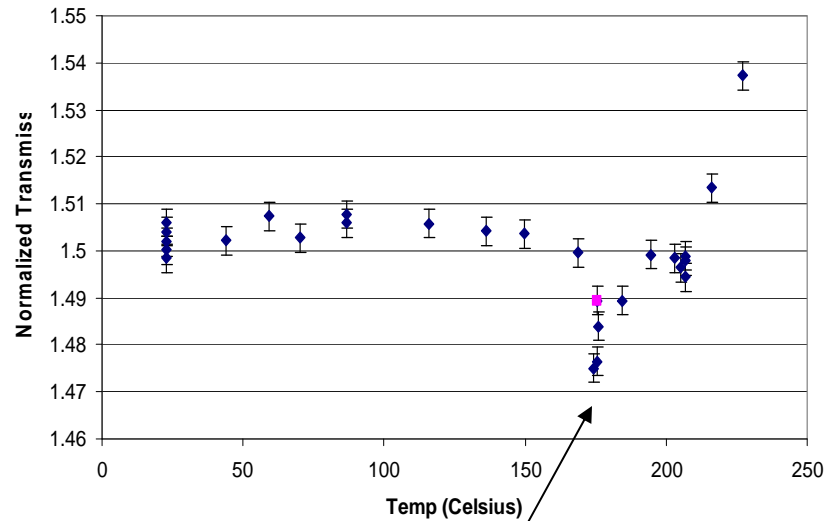
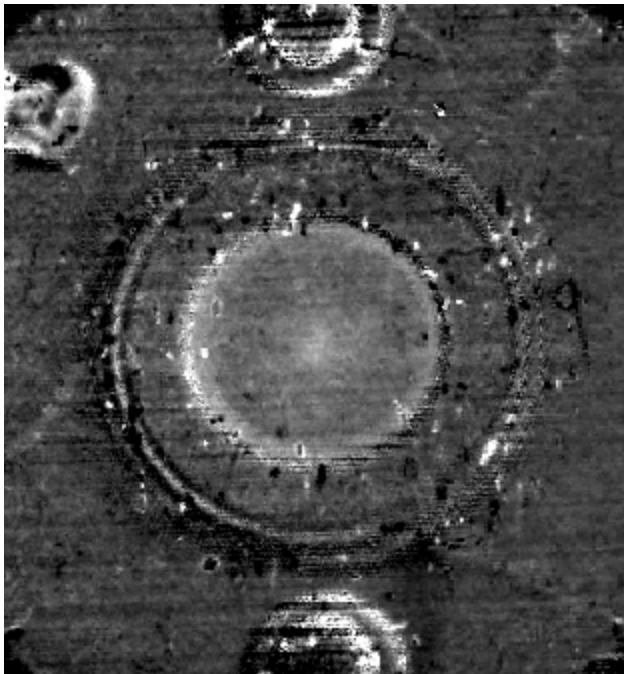
UNCLASSIFIED

EST. 1943

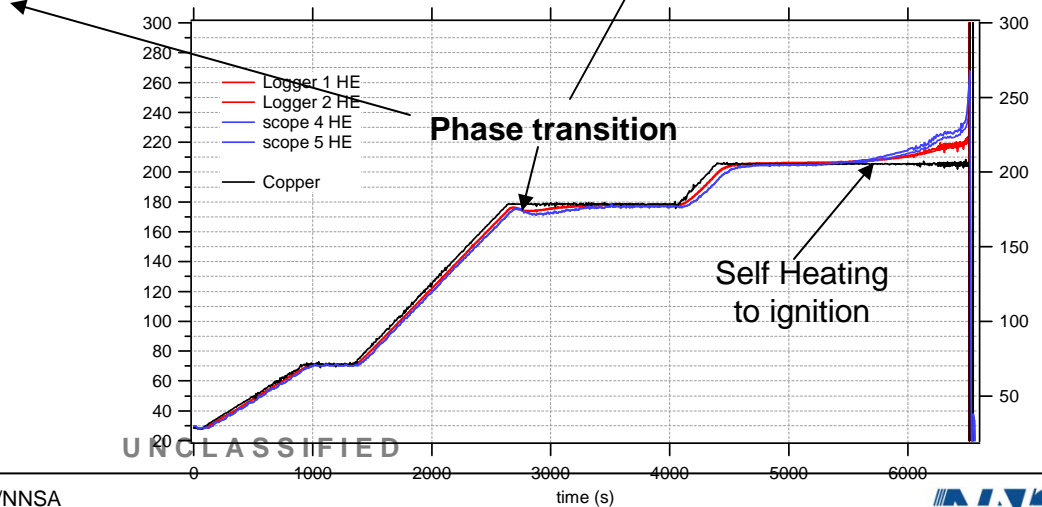
Operated by the Los Alamos National Security, LLC for the DOE/NNSA



Pre-ignition Density Variation

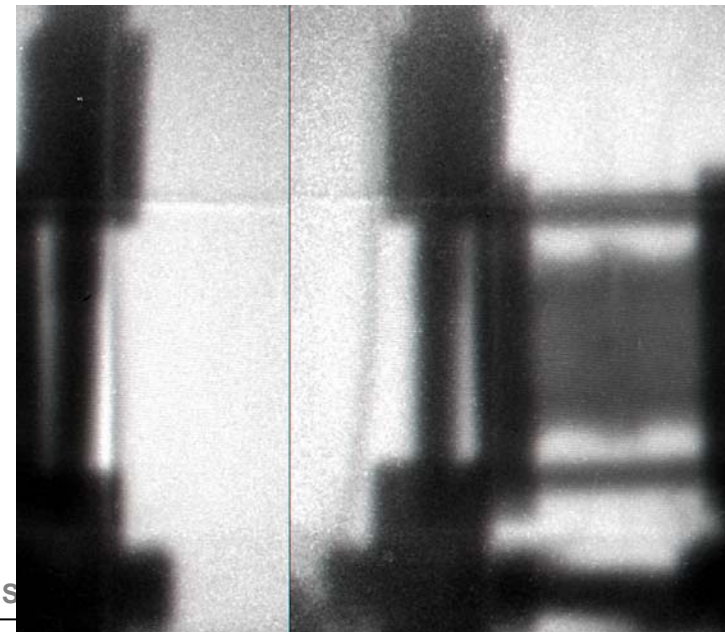
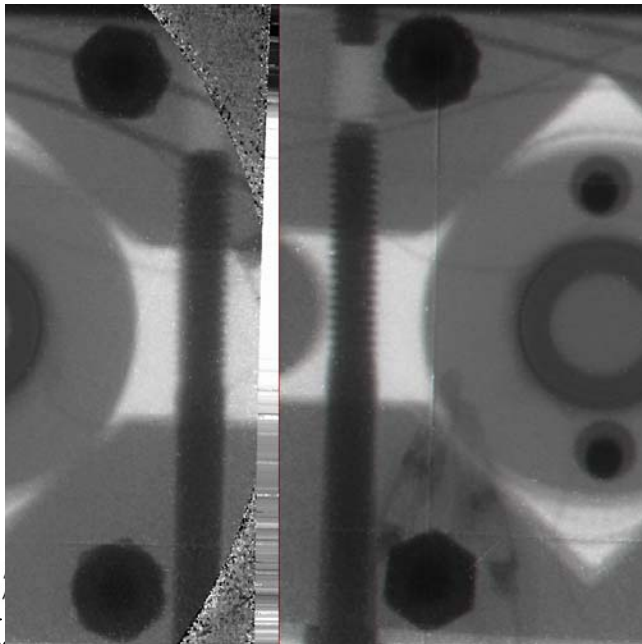
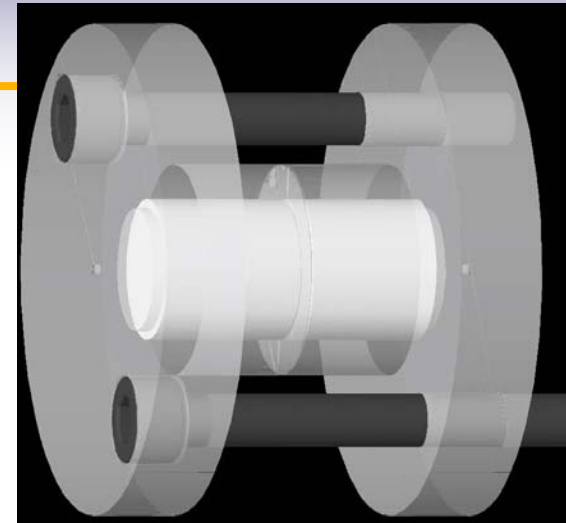


Temperature Ramp



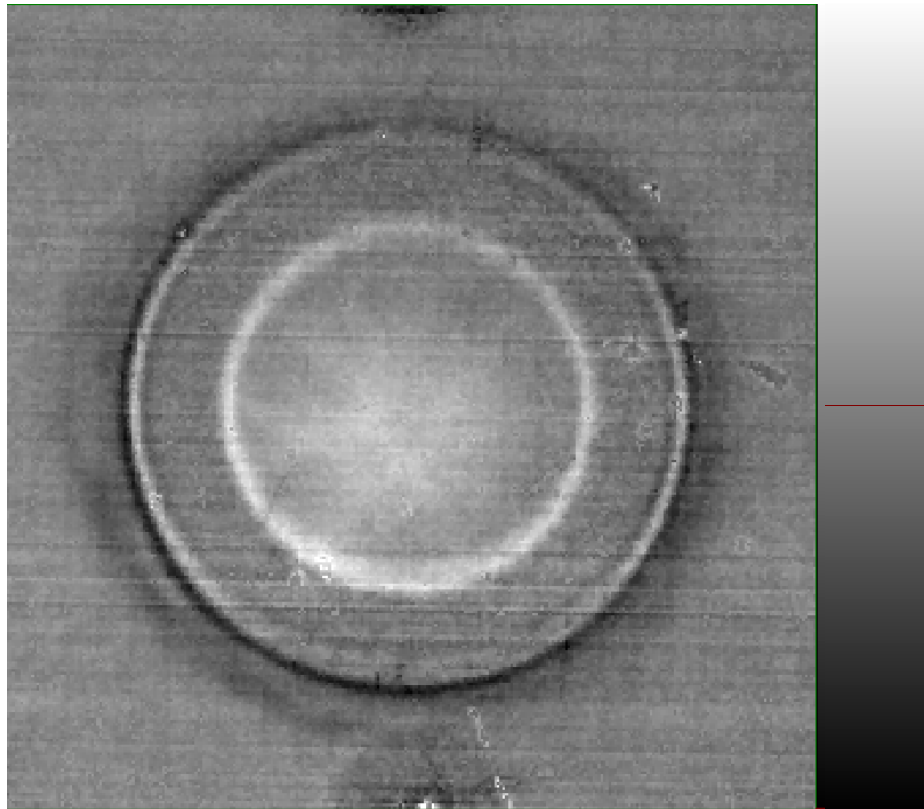
pRad has allowed the mechanism for high explosive cookoff to be elucidated

- Thermal ignition experiment studying properties of PBX-9501 for the surety program
- Proton radiography provides information on:
 - Pre-ignition density variations of HE
 - Ignition propagation
 - Encasing material drive



Ignition Propagation

Transmission Images



1.2

Results

Central ignition

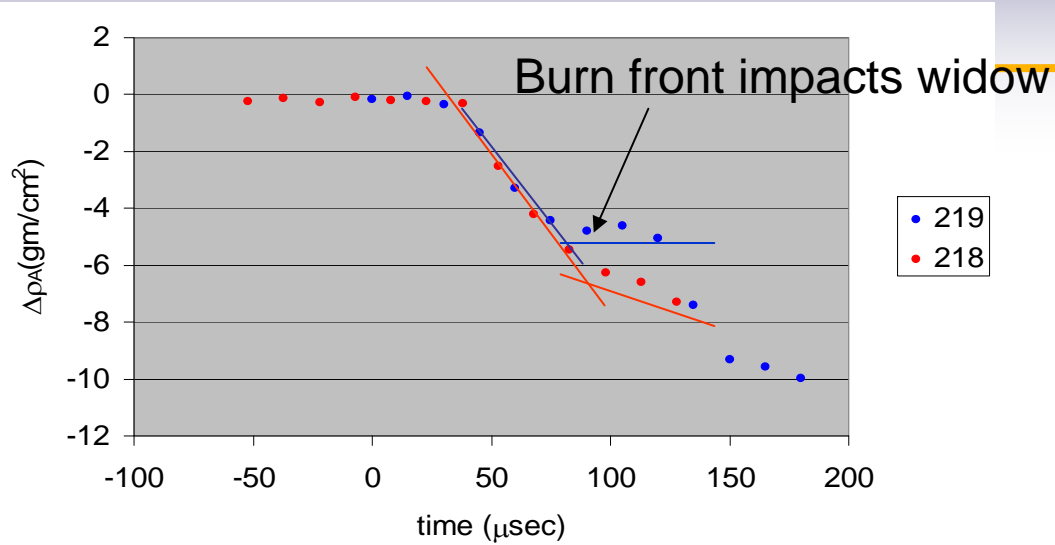
Radial propagation

“star” ignition pattern

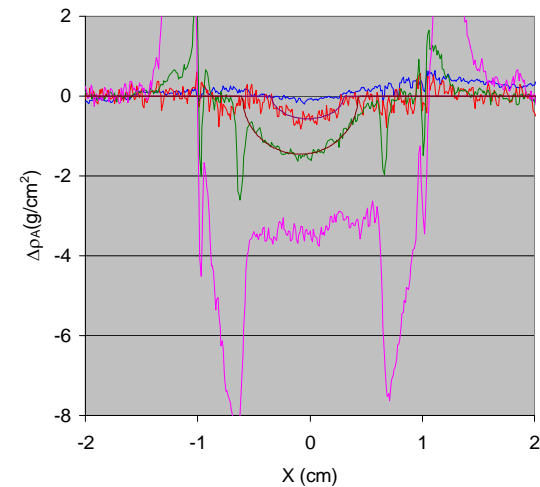
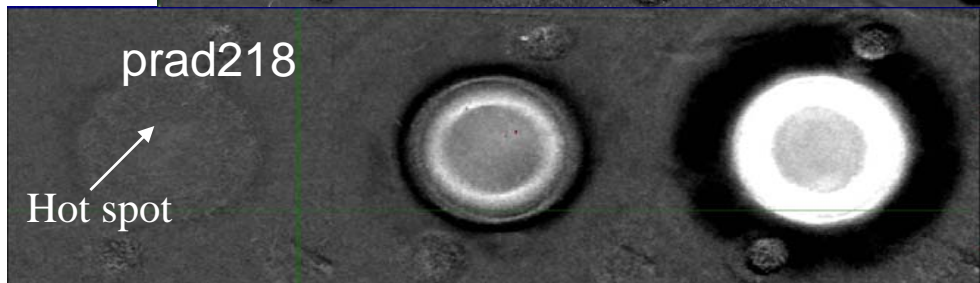
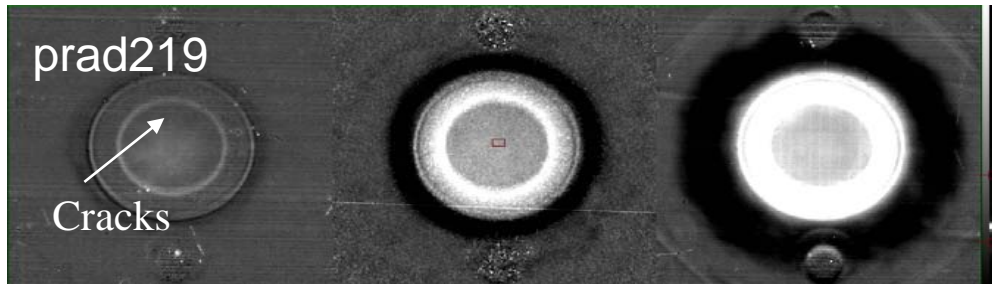
Detailed comparisons
with models ongoing
within C division and P
division

.8

Combining data from two experiment shows features of the ignition mechanisms

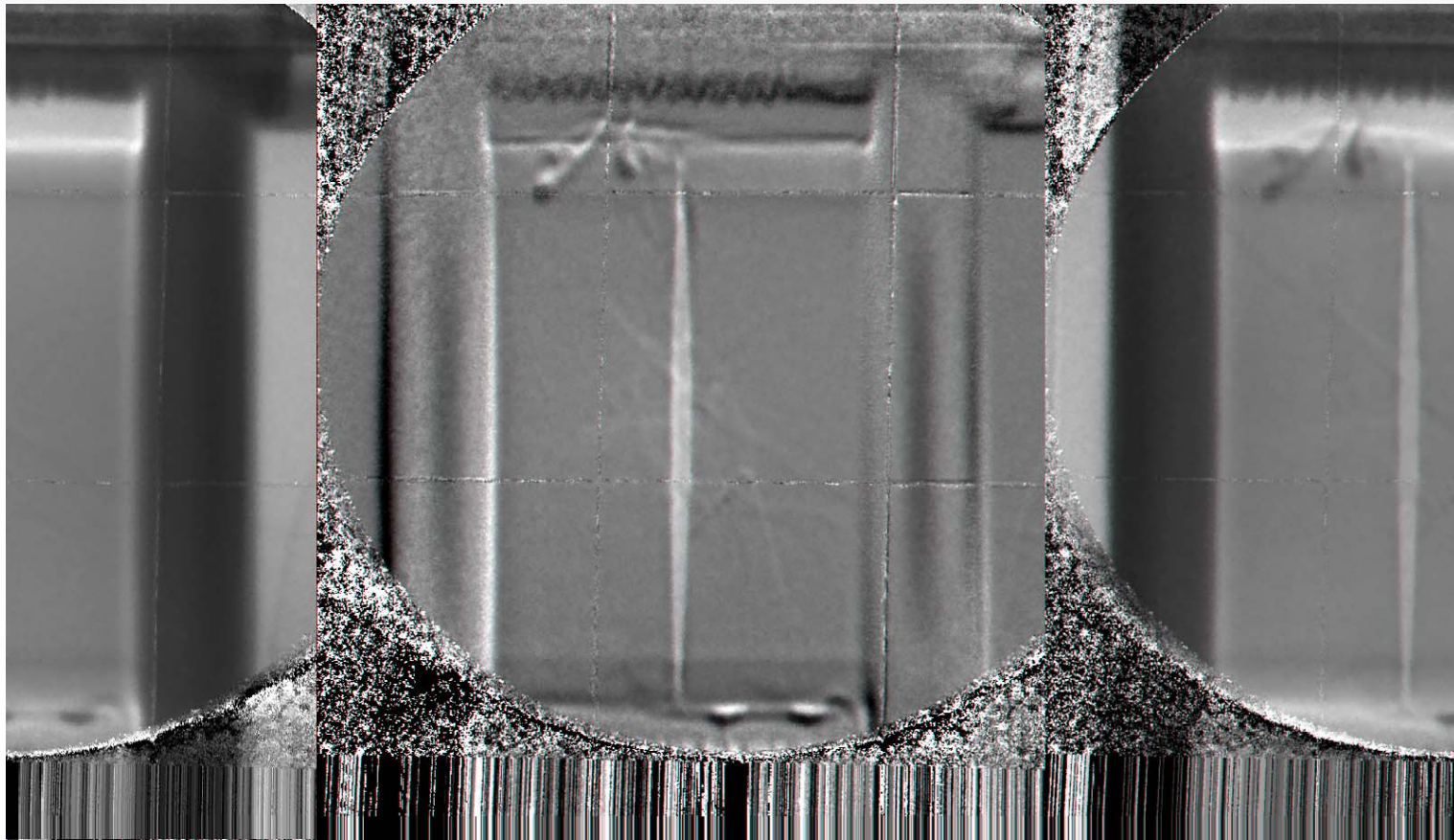


- Hot spot develops
- Ignition propagates along cracks
- Reaction burns remaining material



UNCLASSIFIED

A recent (Aug 7-8th) proton radiography movie shows features of the ignition mechanism



pRad Core Team

P-25

Eduardo Campos, Camilo Espinoza, Gary Hogan, Brian Hollander, Julian Lopez, Fesseha Mariam, Frank Merrill, Christopher Morris, Matthew Murray, Alexander Saunders, Cynthia Schwartz, T. Neil Thompson, Dale Tupa

DE-3

Joe Bainbridge, Robert Lopez, Mark Marr-Lyon, Paul Rightley

HX-4

Wendy McNeil

P-23

Gary Grim, Nicholas King, Kris Kwiatkowski, Paul Nedrow

LANSCE-NS

Leo Bitteker

NSTech

Douglas Lewis, Josh Tybo